

# Dispersion (asymptotic) theory of charged particle transfer reactions at low energies and nuclear astrophysics: II. the asymptotic normalization coefficients and their nuclear-astrophysical application

R. Yarmukhamedov,<sup>1,2\*</sup> K. I. Tursunmakhatov<sup>3</sup> and N. Burtebayev<sup>2,4</sup>

March 13, 2020

<sup>1</sup>*Institute of Nuclear Physics, 100214 Tashkent, Uzbekistan*

<sup>2</sup>*Al Farabi Kazakh National University, 050040 Almaty, Kazakhstan*

<sup>3</sup>*Gulistan State University, 120100 Gulistan, Uzbekistan*

<sup>4</sup>*Institute of Nuclear Physics, 050032 Almaty, Kazakhstan*

## Abstract

Within the asymptotic theory proposed by authors R. Yarmukhamedov and K.I. Tursunmakhatov [Phys. Rev. C (submitted 2019)] for the peripheral sub- and above-barrier transfer  $A(x, y)B$  reaction in the three-body ( $A$ ,  $a$  and  $y$ ) model ( $x = y + a$  and  $B = A + a$ , and  $a$  is a transferred particle), the analysis of the experimental angular distributions of the differential cross sections is performed for the peripheral proton and triton transfer  ${}^9\text{Be}({}^{10}\text{B}, {}^9\text{Be}){}^{10}\text{B}$ ,  ${}^{16}\text{O}({}^3\text{He}, d){}^{17}\text{F}$  and  ${}^{19}\text{F}(p, \alpha){}^{16}\text{O}$  reactions at above- and sub-barrier projectile energies, respectively. New estimates and their uncertainties are obtained for magnitudes of the asymptotic normalization coefficients (respective the nuclear vertex constants) for  ${}^9\text{Be} + p \rightarrow {}^{10}\text{B}$ ,  ${}^{16}\text{O} + p \rightarrow {}^{17}\text{F}$  and  ${}^{16}\text{O} + t \rightarrow {}^{19}\text{F}$ . They are applied for calculations of the astrophysical  $S$  factors for the nuclear-astrophysical  ${}^9\text{Be}(p, \gamma){}^{10}\text{B}$ ,  ${}^{16}\text{O}(p, \gamma){}^{17}\text{F}$  and  ${}^{19}\text{F}(p, \alpha){}^{16}\text{O}$  reactions at thermonuclear energies. New values and their uncertainties are obtained for the astrophysical  $S$  factors at stellar energies.

PACS: 25.60 Je; 26.65.+t

---

\*Corresponding author, E-mail: rakhim@inp.uz

## I. INTRODUCTION

Results from earlier nuclear physics research at very level in a hot Big Bang nucleosynthesis, which were predicted by astrophysicists within the framework of the standard cosmology, led to suspicion that spallation reactions play the main role in production of light elements such as B, O, F and etc. See Refs. [1, 2]. Therefore, a reliable estimation of rates of different nuclear astrophysical processes responsible for the light element abundance is one of the most actual problems of the modern nuclear astrophysics [3]. Solution of this problem is in turn impossible without obtaining rather low energy cross sections  $\sigma(E)$  (or respective astrophysical  $S$  factors  $S(E)$ ) for such reactions.

Despite the impressive improvements in our understanding of such reactions made in the past decades (see Refs [3–6] for example) ambiguities connected both with the extrapolation of the measured cross sections for some specific nuclear-astrophysical reactions above within the stellar energy region and with the theoretical predictions for  $\sigma(E)$  (or  $S(E)$ ) still exist. They may considerably influence predictions of the standard solar model [1, 2]. As a specific example below we consider the nowadays situation concerning the nuclear-astrophysical  ${}^9\text{Be}(p, \gamma){}^{10}\text{B}$ ,  ${}^{16}\text{O}(p, \gamma){}^{17}\text{F}$  and  ${}^{19}\text{F}(p, \alpha){}^{16}\text{O}$  reactions since the calculations of the corresponding astrophysical  $S$  factors, performed within different methods [7–15], show noticeable spread exceeding the experimental errors.

The  ${}^9\text{Be}(p, \gamma){}^{10}\text{B}$  reaction plays an important role as one of the critical links in primordial and stellar nucleosynthesis of light elements in the  $p$  shell [1, 2, 14, 15]. In [14], the experimental astrophysical  $S$  factors ( $S_{19}^{\text{exp}}(E)$ ) for this reaction were measured over the energy range  $68 < E < 125$  keV via the measurement of the branching ratio for the  ${}^9\text{Be}(p, \gamma){}^{10}\text{B}$  and  ${}^9\text{Be}(p, \alpha){}^6\text{Li}$  reactions (here and everywhere below, the lower indexes in the astrophysical  $S$  factor denote mass numbers of the colliding particles). It was revealed that the  $S_{19}^{\text{exp}}(E)$  measured is practically independent from the energy  $E$ . In [14], these data were then analyzed within the framework of the two-body potential method under two the assumptions that the pure direct capture contributes and the spectroscopic factor for the  ${}^{10}\text{B}$  nucleus in the  $({}^9\text{Be} + p)$  configuration can be set equal to unity. On the other hand, the experimental energy dependence of the  $S_{19}^{\text{exp}}(E)$ , measured by authors of Ref. [15] over the range most important to nuclear astrophysics ( $66 < E < 1620$  keV), includes contributions from four the resonances and the direct capture as well as their allowed interference with each other. In [11], the  $S_{19}^{\text{exp}}(E)$  data of Ref. [15] were analyzed within the two-body potential method where the direct component ( $S_{19}^{\text{DC}}(E)$ ) of the calculated total astrophysical  $S$  factor ( $S_{19}(E)$ ) is presented as the product of the spectroscopic factor mentioned above, which is taken from [16], and the bilinear polynomial over the energy  $E$ . The obtained result shows that the calculated  $S_{19}(E)$  values are larger than the results of [14] by a factor of 4.2. In [7], the analysis of the experimental data [15] has been performed within the modified  $R$ -matrix method in which the contribution from the direct capture amplitude to the total  $S_{19}(E)$  is calculated using the “indirect measured” ANC for  ${}^9\text{Be} + p \rightarrow {}^{10}\text{B}$  derived in Ref. [17] for the ground and first three excited states of  ${}^{10}\text{B}$ . In this connection, one notes that, in [17], the ANC’s above were obtained from the analysis of the precisely measured differential cross sections (DCS’s) for the proton exchange  ${}^{10}\text{B}$ - ${}^9\text{Be}$  reaction, which was within the “post” form of the modified distorted-wave Born approximation (MDWBA). Hence, the

contribution of the three-body Coulomb effects in the full transition operator of the three-body DWBA amplitude is taken into account in the first order of the perturbation theory over the Coulomb polarization potential  $\Delta V_{i,f}^C$  [18]. While, as shown in Ref. [19], when the residual  $^{10}\text{B}$  nucleus in the peripheral transfer reaction is formed especially in excited bound states, this restriction over  $\Delta V_{i,f}^C$  in the transition operator does not guarantee the necessary accuracy of the “indirect measured” ANC values for their astrophysical application. Besides, in [7], the channel contribution [20] to the resonance  $\gamma$ -ray width in the resonance component of the total  $R$ -matrix amplitude as a factor, was ingored. Correct taking into account this contribution to the resonance  $\gamma$ -ray width may influence the energy dependence of the resonance amplitude given by Eqs. (5)–(7) in [7]. Therefore, it would be highly encouraged an examination of a degree of a reliability of the assumptions used in Refs. [7, 17].

If the subsequent hydrogen burning of  $^{19}\text{F}$  proceeds predominantly through the  $^{19}\text{F}(p, \alpha)^{16}\text{O}$  reaction, the  $^{16}\text{O}(p, \gamma)^{17}\text{F}$  reaction is the first one in a link of the sequence of a four branch in CNO hydrogen burning proceeding via  $^{16}\text{O}(p, \gamma)^{17}\text{F}(e^+ \nu_e)^{17}\text{O}(p, \gamma)^{18}\text{F}(e^+ \nu_e)^{18}\text{O}(p, \gamma)^{19}\text{F}(p, \alpha)^{16}\text{O}$ . This changeover from the  $pp$ -chain to the CNO cycle is observed near  $T_6 \approx 20$  K (the Gamow’s energy  $E_G \approx 35.2$  keV) [2]. The  $^{16}\text{O}(p, \gamma)^{17}\text{F}$  reaction rate sensitively influences the  $^{17}\text{O}/^{16}\text{O}$  isotopic ratio predicted by models of massive AGB stars, where proton capture occurs at the base of the convective envelop. In second-generation stars, whose stellar temperatures are higher than those for the quiescent CNO cycle, the  $^{19}\text{F}(p, \gamma)^{20}\text{Ne}$  and  $^{19}\text{F}(p, \alpha)^{16}\text{O}$  reactions compete with each other in the hydrogen burning phase corresponding to the transition from the hot CNO cycle to the NeNa one. Furthermore, the  $^{19}\text{F}(p, \alpha)^{16}\text{O}$  reaction can play an important role both in hydrogen-rich environment and in the AGB stars as the main sites of fluorine production [2]. Despite its importance, the astrophysical  $S$  factors have still large uncertainties at astrophysical energies [21]. As it is seen from above, exact knowledge of the rates of the  $^{16}\text{O}(p, \gamma)^{17}\text{F}$  and  $^{19}\text{F}(p, \alpha)^{16}\text{O}$  reactions is of great importance for modeling of nucleosynthesis in the hydrogen-burning massive stars.

There are old measurements of the  $^{16}\text{O}(p, \gamma)^{17}\text{F}$  reaction close to the energy region of astrophysical interest (see [16] and references therein). However, these experiments did not distinguish between transitions into the ground ( $E^*=0.0$ ;  $J^\pi=5/2^+$ ) state and the first excited ( $E^*=0.497$  MeV;  $J^\pi=1/2^+$ ) state of the residual  $^{17}\text{F}$  nucleus. In [22], the experimental astrophysical  $S$  factor,  $S_{16}^{\text{exp}}(E)$ , has been measured in the energy range  $200 \leq E \leq 3750$  keV with the separated ground and first excited states of the residual  $^{17}\text{F}$  nucleus. They were then analyzed using the Woods-Saxon potential in the standard two-body method under the assumption that the spectroscopic factors for  $^{17}\text{F}$  in the  $(^{16}\text{O} + p)$  configuration can be set to unity both for the ground state and for the first excited one of  $^{17}\text{F}$ . However, as shown in [8], in reality, there are infinite number of the phase-equivalent Woods-Saxon potentials resulting in the theoretical uncertainty about 50% in the calculated  $S_{16}(E)$  values at stellar energies. Though, all these potentials lead to the calculated phase shifts for the  $p^{16}\text{O}$ -scattering, which are in a well agreement with the experimental data within the uncertainty up to  $\sim 10\%$ . It follows from here that the results of Ref. [22] derived for  $S_{16}(E)$  are strongly model-dependent. It is mainly associated with the fact that the spectroscopic factors above cannot be determined unambiguously [8] and, so, their values should not be set to unity, a priori. The astrophysical  $S$  factor  $S_{16}(E)$  at stellar energies was also calculated in [23] within the standard two-body

potential method using the ANC values for  $^{16}\text{O} + p \rightarrow ^{17}\text{F}(\text{g.s.})$  and  $^{16}\text{O} + p \rightarrow ^{17}\text{F}(0.497 \text{ MeV})$ . They were derived in [23] from the analysis of the experimental DCS's of the peripheral proton transfer  $^{16}\text{O}(^3\text{He}, d)^{17}\text{F}$  reaction, which was performed within the post form of the modified DWBA. As it was mentioned above, the post form of the modified DWBA cannot provide the necessary accuracy in the ANC values for their astrophysical application, especially, for the very weakly bound first excited state of  $^{17}\text{F}$ . This point relates to the ANC values obtained in Ref. [24] from the analysis of the same peripheral proton transfer reaction in the finite-range of the “post”-approximation of MDWBA. That apparently is one of the reasons why the central value for the square of the ANC for  $^{16}\text{O} + p \rightarrow ^{17}\text{F}(0.497 \text{ MeV})$  recommended in Refs. [23] and [24] is about  $3.5\sigma$  larger and  $2.6\sigma$  lesser, respectively, than that recommended in Refs. [8, 25]. See Table 1 below.

For the  $^{19}\text{F}(p, \alpha)^{16}\text{O}$  reaction there are unpublished experimental data by Lorenz-Wirzba [26] and the data measured by authors of Refs. [9] at the lowest sub-barrier proton projectile energies, including nonresonant values ( $\lesssim 500 \text{ keV}$ ). The experimental angular distributions of the differential cross sections of Ref. [26] measured at the proton projectile energies 250, 350 and 450 keV have been quoted in Ref. [27], where the analysis has been performed within the zero-range approximation of the conventional DWBA. As a consequence, it was revealed that the ground state transition may be dominated by a direct mechanism in the nonresonant energy region below the Coulomb barrier, involving the vicinity of the AGB Gamow window ( $\simeq 27\text{--}94 \text{ keV}$  at  $T_6 \simeq 40 \text{ K}$ ). Nevertheless, it occurs the discrepancy between the absolute values of the experimental angular distributions of Refs. [26] and [9] at rather close nonresonant proton projectile energies by a factor of about 2. Besides, the results of the investigation of the  $^{19}\text{F}(p, \alpha)^{16}\text{O}$  reaction at energies below the Coulomb barrier reported by different authors (see recent work of Ref. [9] and references therein) show a presence of rather large spread in the calculated values of the astrophysical  $S$  factors at center-of-mass energies down 200 keV. Therefore, the application of the asymptotic theory developed in Ref. [19] for the sub-barrier  $^{19}\text{F}(p, \alpha)^{16}\text{O}$  reaction allows to obtain new quantitative information both about the direct mechanism at nonresonant projectile energies and about the possibility of extraction of the “indirect determined” ANC for  $^{16}\text{O} + t \rightarrow ^{19}\text{F}$ .

Below, we present the results of the analysis of the experimental angular distributions of the DCS's for the mentioned above peripheral proton and triton transfer reactions [17, 23, 26, 9] and their application for obtaining a new information about the extrapolated astrophysical  $S$  factors at stellar energies for the corresponding specific nuclear-astrophysical processes. The analysis will be performed within framework of the asymptotic theory developed in Ref. [19] since all these reactions are related to the “non-dramatic” case. As noted in Refs. [18, 19], the latter occurs when the values of the Coulomb parameters for the two-body bound state wave functions in the entrance and exit channels or their sum are not in the vicinity of a natural number.

## VI. ANALYSIS OF THE PERIPHERAL SUB- AND ABOVE-BARRIER TRITON AND PROTON REACTIONS

In this section, we present the results of comparison of the calculated DCS's with experimental data for the following peripheral proton and triton transfer reactions:

- (I)  ${}^9\text{Be}({}^{10}\text{B}, {}^9\text{Be}){}^{10}\text{B}$  at the  ${}^{10}\text{B}$  incident energy  $E_{i0\text{B}}=100$  MeV [17],  
 (II)  ${}^{16}\text{O}({}^3\text{He}, d){}^{17}\text{F}$  at  $E_{3\text{He}}=29.75$  MeV [23],  
 (III)  ${}^{19}\text{F}(p, \alpha){}^{16}\text{O}$  [9, 26] at six sub-barrier proton projectile energies.

The experimental angular distributions of the DCS's of the reaction (I) are analyzed for the residual  ${}^{10}\text{B}$  nucleus populating the ground ( $E^*=0.0$ ;  $J^\pi=3^+$ ) state, the first ( $E^*=0.718$  MeV;  $J^\pi=1^+$ ), second ( $E^*=1.740$  MeV;  $J^\pi=0^+$ ) and third ( $E^*=2.154$  MeV;  $J^\pi=1^+$ ) excited states (denoted by  ${}^{10}\text{B}_0$ ,  ${}^{10}\text{B}_1$ ,  ${}^{10}\text{B}_2$  and  ${}^{10}\text{B}_3$ , respectively, below). The residual  ${}^{17}\text{F}$  nucleus in the reaction (II) is formed in the ground ( $E^*=0.0$ ;  $J^\pi=\frac{5}{2}^+$ ) and first ( $E^*=0.495$  MeV;  $\frac{1}{2}^+$ ) excited states (denoted by  ${}^{17}\text{F}_0$  and  ${}^{17}\text{F}_1$ , respectively, below). For the reaction (III) populating the ground state of the residual  ${}^{16}\text{O}$  nucleus, two the sets of the independently measured experimental data are considered, which correspond to the projectile proton energy ( $E_p=250$ ; 350 and 450 keV [26] (denoted by EXP-1978 below) and  $E_p=327$ ; 387 and 486 keV [9] (denoted by EXP-2015 below).

For the reactions considered above, the orbital  $l_B$  and  $l_x$  angular momentums of the transfer  $a$  particle ( $a$  is either proton or triton) in the bound  $B$  and  $x$  nuclei ( $B$  is either  ${}^{10}\text{B}_i$  or  ${}^{17}\text{F}_i$  or  ${}^{19}\text{F}$  and  $x$  is either  ${}^{10}\text{B}_0$  or  ${}^3\text{He}$  or  $\alpha$  particle), respectively, are taken equal to  $l_{i0\text{B}_i}=1$  ( $i=0-3$ ),  $l_{17\text{F}_0}=2$  and  $l_{17\text{F}_1}=l_{19\text{F}}=0$ , and  $l_{3\text{He}}=l_\alpha=0$ . Since the energy of incident  ${}^3\text{He}$  in the reaction (II) is moderate, the contribution of the  $d$ -state of the  ${}^3\text{He}$  nucleus in the vertex  ${}^3\text{He} \rightarrow d + p$  is neglectable small [28]. In this case, the total angular  $j_B$  and  $j_x$  momentums, where  $\mathbf{j}_B = \mathbf{l}_B + \mathbf{J}_a$  and  $\mathbf{j}_x = \mathbf{l}_x + \mathbf{J}_a$  in which  $\mathbf{J}_a$  is the spin of the transferred  $a$  particle, are taken equal to  $j_{i0\text{B}_0}=j_{i0\text{B}_2}=3/2$ ,  $j_{17\text{F}_0}=5/2$ ,  $j_{19\text{F}}=1/2$ , and  $j_{17\text{F}_1}=j_\alpha=j_{3\text{He}}=1/2$ , whereas  $j_{i0\text{B}_1}=j_{i0\text{B}_3}=1/2$  and  $3/2$ .

In this case, at the fixed values of the angular ( $l_x$  and  $l_B$ ) and total ( $j_x$ ) orbital momentums defined above, the expression (51), derived in Ref. [19] for the DCS of the peripheral transfer  $A(x, y)B$  reaction (where  $B = A + a$  and  $x = y + a$ , and  $a$  is the transferred particle), can be presented in the form

$$\frac{d\sigma}{d\Omega} = C_x^2 \sum_{j_B} C_{B;j_B}^2 \tilde{\sigma}_{r_0}(j_B; E_i, \theta), \quad (1)$$

where  $C_{B;j_B} = C_{Aa;l_B j_B}$  and  $C_x = C_{ay;l_x j_x}$  are the ANC's for  $A + a \rightarrow B$  and  $y + a \rightarrow x$  [28], respectively, which are related to respective the nuclear vertex constants (NVCs) for the virtual decays  $B \rightarrow A + a$  and  $x \rightarrow y + a$  by the simple relations given in [28] (see Eq. (7) in [19] also); the  $\tilde{\sigma}_{r_0}(j_B; E_i, \theta)$  is a known function of the center-of-mass scattering angle  $\theta$  and energy  $E_i$  at fixed values of the quantum ( $l_x, j_x, l_B$ ) numbers above and the cut-off channel  $R_i^{\text{ch}}$  and  $R_f^{\text{ch}}$  radii corresponding respectively to the entrance and exit channels. They enter the lower limits of the radial integral of the matrix element of the reaction and can be determined by  $R_i^{\text{ch}}=r_0(A^{1/3} + x^{1/3})$  and  $R_f^{\text{ch}}=r_0(B^{1/3} + y^{1/3})$ , where  $r_0$  is the nuclear interaction radius and  $D$  is a mass number of  $D$  nucleus ( $D = A, x, B$  and  $y$ ). The optical potentials for the entrance and exit channels were taken from Refs. [17, 23] (the sets 1 and 2) and [27]. Calculations were performed using the expression (51) of [19] and Eq. (1) in which the influence of the three-body ( $A, a$  and  $y$ ) Coulomb dynamics of the transfer mechanism on the peripheral partial amplitudes at  $l_i \gg 1$  and  $l_f \gg 1$  of the reaction amplitude is taken into account in a correct manner. As shown in [19], this influence on the amplitudes of the reactions considered above is

also noticeable at least in the angular range of the main peak of the angular distributions. It is also related to the calculated reduced  $\tilde{\sigma}_{r_0}(j_B; E_i, \theta)$  cross sections. The values of the product of the square of the ANC's above and  $r_0$  entering Eq. (1) and their uncertainties giving the best fit to the experimental DCS's within the experimental errors have been defined by minimizing the quantity  $\chi^2$  in the fitted data only in the angular region of the main peak of the angular distribution.

### A. Asymptotic normalization coefficients for ${}^9\text{Be} + p \rightarrow {}^{10}\text{B}$ , ${}^{16}\text{O} + p \rightarrow {}^{17}\text{F}$ and ${}^{16}\text{O} + t \rightarrow {}^{19}\text{F}$

Figs. 1 – 3 show the results of the calculations of the DCS's obtained in the present work (the solid curves), their comparison with the conventional DWBA calculations performed in Refs. [17, 23, 27] (the dash curves) and experimental data. The results of the present work correspond to the standard value of the  $r_0$  parameter, which is taken equal to 1.25 fm and also to the minimum of  $\chi^2$  in the angular region of the main peak of the angular distribution. It is seen that the angular distributions calculated in the present work reproduce equally well the experimental data in the angular range of the main peak of the corresponding angular distributions. The square of the ANC values and that of the modules of the respective NVC ones ( $|G_B|^2$ ) are summarised in Table 1. They are found by normalizing the calculated cross sections to the corresponding experimental ones at the forward angles and using the ANC's  $C_{{}^3\text{He}}^2 = 4.20 \pm 0.32 \text{ fm}^{-1}$  ( $|G_{{}^3\text{He}}|^2 = 1.32 \pm 0.10 \text{ fm}$ ) for  $d + p \rightarrow {}^3\text{He}$  compiled in [29] and  $C_\alpha^2 = 54.2 \pm 4.5 \text{ fm}^{-1}$  [30] ( $|G_\alpha|^2 = 13.4 \pm 1.1 \text{ fm}$ ) for  $t + p \rightarrow \alpha$ . There, the theoretical and experimental uncertainties correspond to variation (up to  $\pm 3.0\%$ ) of the  $r_0$  parameter with respect to its standard value above and the experimental errors in  $d^{\text{exp}}\sigma/d\Omega$ , respectively. The experimental uncertainties pointed out in the ANC (NVC) values for  ${}^{17}\text{F} \rightarrow {}^{16}\text{O} + p$  and  ${}^{19}\text{F} \rightarrow {}^{16}\text{O} + t$  correspond to the average squared errors, which includes both the experimental errors in  $d^{\text{exp}}\sigma/d\Omega$  and the above-mentioned uncertainty of the ANC (NVC) for  $d + p \rightarrow {}^3\text{He}$  and  $t + p \rightarrow \alpha$ , respectively. One notes that the value of  $C_{{}^3\text{He}}^2$  ( $|G_{{}^3\text{He}}|^2$ ) above is in an excellent agreement within its uncertainty with the “indirect measured” (“experimental”) values of  $4.28 \pm 0.50 \text{ fm}^{-1}$  ( $1.34 \pm 0.15 \text{ fm}$ ) [8] and  $4.35 \pm 0.10 \text{ fm}^{-1}$  ( $1.36 \pm 0.03 \text{ fm}$ ) [31], which were obtained from the independent indirect methods. Therefore, they can be considered as the most reliable ones so far.

As is seen from the first – ninth lines of Table 1, the  $C_{{}^{10}\text{B}_0}^2$  value for  ${}^9\text{Be} + p \rightarrow {}^{10}\text{B}_0$  obtained in the present work differs noticeably from that of [17] derived from the analysis of the same reaction performed within the framework of the “post” form of the modified DWBA. This difference exceeds overall the normalization accuracy ( $\Delta_{\text{exp}} = 7\%$  [17]) for the absolute values of the DCS's. While, such the difference for the  $C_{{}^{10}\text{B}_0}^2$  derived in [17] (the third and sixth lines) exceeds the  $\Delta_{\text{exp}}$  error and is about of 9%. The central value of the weighed mean of the square of the ANC for  ${}^9\text{Be} + p \rightarrow {}^{10}\text{B}_0$  ( $C_{{}^{10}\text{B}_0}^2 = 4.35 \pm 0.28 \text{ fm}^{-1}$ ) recommended in the present work is  $2.5\sigma$  lower than that of [17] presented in the ninth line of Table 1. One notes that our result for the weighed  $C_{{}^{10}\text{B}_0}^2$  mean value has overall the uncertainty of about 6%. Therefore, the value of  $C_{{}^{10}\text{B}_0}^2$  above is used by us for obtaining the ANC's  $C_{{}^{10}\text{B}_i}^2$  for  ${}^9\text{Be} + p \rightarrow {}^{10}\text{B}_i$  ( $i=1-3$ ). The results for  $C_{{}^{10}\text{B}_i}^2$  and their comparison with those obtained by other authors are presented in the tenth–fifty fourth lines of Table 1. In Table 1, the weighed  $C_{{}^{10}\text{B}_i}^2$  mean

values recommended in the present work are listed in the eighteenth and twenty eighth lines ( $C_{10B_1}^2 = 1.39 \pm 0.09$  and  $3.74 \pm 0.32 \text{ fm}^{-1}$  for  $j_{10B_1} = 1/2$  and  $3/2$ , respectively), thirty eighth line ( $C_{10B_2}^2 = 3.58 \pm 0.34 \text{ fm}^{-1}$  for  $j_{10B_2} = 3/2$ ) and the forty eighth and fifty seventh lines ( $C_{10B_3}^2 = 0.25 \pm 0.06$  and  $0.72 \pm 0.19 \text{ fm}^{-1}$  for  $j_{10B_3} = 1/2$  and  $3/2$ , respectively). There, as a comparison with the results of the present work, the results of Ref. [17] are listed, which were derived using the  $C_{10B_0}^2$  value presented in the ninth line. Note once more that this value is overestimated with respect to that obtained in the present work. As is seen from Table 1, the similar difference occurs between our results and those obtained in [17] for the  $C_{10B_i}^2$  ANC's ( $i=1-3$ ), which is up to  $\sim 19\%$  for the second excited state of the residual  $^{10}\text{B}$  nucleus. This means that the contribution of the three-body ( $^9\text{Be}$ ,  $p$  and  $^9\text{Be}$ ) dynamics in the main pole proton transfer mechanism enhances for the excited states of  $^{10}\text{B}$  populating in the entrance channel. Besides, as seen from Table 1, the quite notice discrepancy occurs between the results of the present work and those of Ref. [24] obtained from the  $^9\text{Be}(^3\text{He}, d)^{10}\text{B}$  performed within the framework of the “post”-approximation of the conventional DWBA. Therefore, it is difficult to estimate an accuracy of the  $C_{10B_i}^2$  values ( $i=1-3$ ) derived in [17, 24].

The weighed mean values for the square of the ANC's for  $^{16}\text{O} + p \rightarrow ^{17}\text{F}_0$  and  $^{16}\text{O} + p \rightarrow ^{17}\text{F}_1$ , derived in the present work from the analysis performed for the sets 1 and 2 of the optical potentials, are presented in the sixty seventh and eighty first lines of Table 1, respectively. As is seen from there, the noticeable dependence of the  $C_{17F_i}^2$  values ( $i=1$  and  $2$ ) from the used sets for the optical potentials is observed both for the results of the present work and for those of Ref. [23]. Nevertheless, as noted above, the results of Ref. [23] have been obtained with the underestimated  $C_{3\text{He}}^2$  value for  $d + p \rightarrow ^3\text{He}$  given in [32]. Besides, the considerable discrepancy occurs between the results of the present work and those of Refs.[12] and [24] obtained within the continuation method for the experimental  $p^{16}\text{O}$ -scattering function and the  $^{16}\text{O}(^3\text{He}, d)^{17}\text{F}$  DCS analysis performed within the finite range of the “post”-approximation of the modified DWBA, respectively. By using this case, one notes that there are misprints in the first line of Table I of Ref. [12]. There, the figures of  $75.5 \pm 15$  and  $1.1 \pm 0.33 \text{ fm}^{-1/2}$  corresponding respectively for the ANC's for  $^{16}\text{O} + p \rightarrow ^{17}\text{F}_1$  and  $^{16}\text{O} + p \rightarrow ^{17}\text{F}_0$  must be replaced by  $75.5 \pm 1.5$  and  $1.04 \pm 0.05 \text{ fm}^{-1/2}$ , respectively. Nevertheless, as is seen from Table 1, our results for the  $C_{17F_i}^2$  above are in good agreement within about  $1\sigma$  with those of Refs. [8] and [25], which were derived by the quite other “indirect” methods.

The  $C_{19F}^2$  values for  $^{16}\text{O} + t \rightarrow ^{19}\text{F}$  obtained in the present work at the different proton projectile energies and their weighted means are presented the eighty eighth – ninety eighth lines of Table 1. As it is seen from there, the weighted  $C_{19F}^2$  mean values found separately from the analysis of the experimental data taken from Ref. [26] (EXP-1978) and from Ref. [9] (EXP-2015), which are listed in the ninety third and ninety eighth lines of Table 1, respectively, differ from each other on the average by a factor of about 2.2. This is the result of the discrepancy between the absolute values of the experimental DCS's of the EXP-1978 and the EXP-2015 measured independently at fairly close energies. To find out the main reason of this discrepancy, we recommend decisive measurement of the experimental DCS's of the  $^{19}\text{F}(p, \alpha)^{16}\text{O}$  reaction in the sub-barrier projectile energy region being closer to that of Refs. [9, 26]. Nevertheless, one notes that the  $C_{19F}^2$  value obtained separately from the independent experimental data of the EXP-1978 and EXP-2015 at the different projectile energies are stable, although the abso-

lute values of the corresponding experimental DCS's of the EXP-1978 and EXP-2015 depend strongly on the proton projectile energy (see Fig. 3). This result confirms the assumption made in Ref. [19] about possibility of the applicability of the asymptotic theory developed in [19] also for the sub-barrier peripheral charged-particle transfer reactions as a tool of obtaining the ANC. To best of our knowledge, the ANC value for  $^{16}\text{O} + t \rightarrow ^{19}\text{F}$  presented in Table 1 are obtained for the first time.

As it is seen from the analysis performed above, the asymptotic theory proposed in Ref. [19] provides better accuracy for the ANC values for  $^9\text{Be} + p \rightarrow ^{10}\text{B}$  and  $^{16}\text{O} + p \rightarrow ^{17}\text{F}$  than those obtained in Refs. [17, 23, 24] for their nuclear-astrophysical application. Besides, the ANC values for  $^{16}\text{O} + t \rightarrow ^{19}\text{F}$  derived above can give a valuable information about the astrophysical  $S$  factors (or the cross sections) for the  $^{19}\text{F}(p, \alpha)^{16}\text{O}$  reaction in the astrophysically relevant energy region where the direct transfer mechanism is dominant. This issue is considered below.

## B. Astrophysical $S$ factors at stellar energies

Here the weighted mean values of the ANC's obtained by us for  $^9\text{Be} + p \rightarrow ^{10}\text{B}_i$  ( $i=0-3$ ) and  $^{16}\text{O} + p \rightarrow ^{17}\text{F}_i$  ( $i=0$  and 1) are used to calculate the astrophysical  $S$  factors for the radiative capture  $^9\text{Be}(p, \gamma)^{10}\text{B}$  and  $^{16}\text{O}(p, \gamma)^{17}\text{F}$  reactions at stellar energies. The calculations are performed within the framework of the modified  $R$ -matrix method (see Ref. [33] for example) for the radiative capture  $^9\text{Be}(p, \gamma)^{10}\text{B}$  reaction, where the direct component of the total amplitude is determined by solely the ANC values, and of the modified two-body potential method (MTBPM) [34] for the direct radiative capture  $^{16}\text{O}(p, \gamma)^{17}\text{F}$  reaction, where the direct astrophysical  $S$  factor is parameterized in the term of the square of the ANC's above. For easier reading of the paper, the basic formulas of these methods are given in Appendix. Besides, the ANC's derived for  $^{16}\text{O} + t \rightarrow ^{19}\text{F}(\text{g.s.})$  are used for getting information about the astrophysical  $S$  factors of the nuclear-astrophysical  $^{19}\text{F}(p, \alpha)^{16}\text{O}$  reaction at six the proton energies mentioned above by means of the way presented in Appendix.

The analysis of the experimental astrophysical  $S$  factors for the  $^9\text{Be}(p, \gamma)^{10}\text{B}$  reaction was performed by taking into account the contributions from captures to fours the resonances and to the direct capture as well as their interference contributions. One notes that three from these resonances are broad ones at  $E_1^{(\text{R})}=287$  keV with  $J^\pi=1^-$ ,  $E_2^{(\text{R})}=892$  keV with  $J^\pi=2^+$  and  $E_4^{(\text{R})}=1161$  keV with  $J^\pi=2^-$ , and one from them is narrow resonance at  $E_3^{(\text{R})}=975$  keV with  $J^\pi=0^+$  [35]. As in Refs. [7, 15], we consider the following transitions from the resonant states above to the ground and three first excited bound states of the residual  $^{10}\text{B}$  nucleus: the  $0^+$  third resonance  $\rightarrow$  the first ( $1^+$ ) and third ( $1^+$ ) bound excited states of  $^{10}\text{B}$ ; the first ( $1^-$ ), second ( $2^+$ ) and fourth ( $2^-$ ) resonances  $\rightarrow$  all the considered bound (ground-excited) states of  $^{10}\text{B}$ . The calculation is performed using Eqs. (A1)–(A8) given in Appendix. As is seen from Eq. (A8), the power of the direct amplitude of the total amplitude given by Eq. (A4) is determined only the  $C_{^{10}\text{B}_i}$  ANC's found above, which will be used in calculations below. Besides, as is seen from Eqs. (A3) and (A4) of Appendix, the direct and resonance terms with the same channel spin ( $I=1$  or 2) interfere only with each other. The calculations show that the resonant and direct amplitudes are formed predominantly by the  $p^9\text{Be}$ -scattering  $s$  wave



capture and the  $E1$  capture, respectively. The direct  $M1$  and  $E2$  contributions into the direct amplitude for all the transitions in the exit channel are negligibly small with respect to the dominant  $E1$  contribution. Hence, they can be ignored.

Fig. 4 shows the results of the calculations for the total ( $S_{19}(E)$  plotted by the solid curve) and direct ( $S_{19}^{\text{DC}}(E)$  plotted by the dashed curve) astrophysical  $S$  factors, which are in an excellent agreement with the experimental data [15]. This is connected apparently with the correct taking into account of the energy dependence of the  $\gamma$ -width, which contains both the interior contribution and the channel one defined by Eq. (A6b) of Appendix. As seen from Fig. 4, the noticeable difference occurs between the direct component of  $S_{19}(E)$  derived in Ref. [7] (the dashed-dotted line) and that obtained in the present work (the dashed line). See also the inset there. Their ratio changes from 1.10 to 1.14 with an increase of the energy  $E$ . This is due to the overestimated values of the ANC's compared to those of the present work (see Table 1). The fitted parameters of all the resonance levels are given in Table 5. The value of the channel radius  $r_c$  ( $r_c = 3.1$  fm) is chosen to provide the minimum of  $\chi^2$  ( $\chi^2=2.5$ ) in fitting data, which is noticeably less than that ( $\chi^2=7.8$ ) obtained in Ref.[7]. In the calculations, the  $\gamma$ -widths of the resonances were considered as adjustable parameters. The protonic- and  $\alpha$ -channel widths for the ground and first three excited states of  $^{10}\text{B}$  are taken from Ref. [35]. As is seen from Table 5, the absolute values of the  $\gamma$ -widths for the first, second and fourth resonances found in the present work by using Eq. (A7), are in good agreement with the results of [35], except for the  $\gamma$ -width for the third ( $0^+$ ) resonance. The  $\gamma$ -width value for the  $0^+$  resonance is found to be  $\Gamma^\gamma=6.5$  eV, which differs about 31% from that ( $\Gamma^\gamma = 8.5$  eV) recommended in [35]. Note that, in [7], all the  $\gamma$ -width values were fixed and taken from [35]. As is seen from Fig. 4, the calculated total astrophysical  $S$  factor reproduces fairly good the experimental data. In particular, the  $S_{19}(0)=0.946\pm 0.194$  keV·b and  $S_{19}^{\text{DC}}(0)= 0.331\pm 0.021$  keV·b as well as  $S_{19}(25 \text{ keV})= 0.970\pm 0.200$  keV·b and  $S_{19}^{\text{DC}}(25 \text{ KeV})= 0.327\pm 0.021$  keV·b are obtained. The value  $S_{19}^{\text{DC}}(0)$  derived in the present work is  $2.5\sigma$  lower than that of  $S_{19}^{\text{DC}}(0)= 0.38\pm 0.02$  keV·b [7, 11]. This difference is associated with the model assumptions used in Refs. [7, 11]. Nevertheless, our result derived for the total  $S_{19}(0)$  is in good agreement with that of  $S(0)=0.96\pm 0.02$  keV·b,  $S(0)=0.96\pm 0.06$  keV·b and  $S_{19}(0)=1.0\pm 0.1$  keV·b derived in Refs. [11], [7] and [15], respectively.

The calculations of the astrophysical  $S$  factors for the direct radiative capture  $^{16}\text{O}(p, \gamma)^{17}\text{F}$  reaction are done by using Eq. (A9) of Appendix. In Eq. (A9), the weighted mean values of the  $C_{17\text{F}_i}^2$  ANC's ( $i=1$  and  $2$ ) for  $^{16}\text{O} + p \rightarrow ^{17}\text{F}_1$  and  $^{16}\text{O} + p \rightarrow ^{17}\text{F}_0$  derived in the present work are used. Whereas, the  $\mathcal{R}_{17\text{F}_j}(E; b_{17\text{F}_j})$  function is calculated similarly to that as is done in Ref. [8]. Nevertheless, we note only the following. The direct amplitude of the reaction above is formed predominantly through the  $E1$ ,  $M1$  and  $E2$  capture. For the transition to the ground ( $^{17}\text{F}_0$ ) state, the  $p$ ,  $f(d)$  waves and the  $s$  and  $d$  ones correspond respectively to the  $E1(M1)$  and  $E2$  transitions. For the transition to the first ( $^{17}\text{F}_1$ ) excited state, the  $p(s)$  wave and the  $d$  wave correspond respectively to the same transitions above. Besides, as shown in [8], the uncertainty of the calculated  $\mathcal{R}_{17\text{F}_j}(E; b_{17\text{F}_j})$  function is about  $\pm 4\%$ . It arises under the variation of the free  $b_{17\text{F}_j}(r_0, a)$  parameter relatively its value corresponding to the standard ( $r_0=1.25$  fm and  $a=0.65$  fm) values of the geometric parameters of the adopted Woods-Saxon potential. Note

that this potential is used for calculating both the bound  $^{17}\text{F}_j$  state wave function and the continuum  $p^{16}\text{O}$ -scattering one, which enter the radial integral of the matrix element [34].

The results of comparison between the astrophysical  $S$  factors ( $S_{116}(E)$ ) calculated in the present work and the experimental data [22] are displayed in Fig. 5. There, the solid curves in (a) and (b) present the results for the ground and first excited states of the residual  $^{17}\text{F}$  nucleus, respectively, whereas the solid curve in (c) corresponds to their sum  $^{17}\text{F}(\text{g.s.} + 0.429 \text{ MeV})$ . In Fig. 5, the width of the bands are the uncertainties, which are the average squared errors of the uncertainties of the ANC's given in Table 1 and that of the  $\mathcal{R}_{l_{17}\text{F}_j}$  function mentioned above, and the dashed curves are the results of Ref. [8]. As is seen from figure, the weighted  $C_{17\text{F}_i}^2$  mean values derived in the present work firstly, reproduce well the experimental data and, secondly, allow extrapolation of the astrophysical  $S$  factors ( $S_{116}(E)$ ) at stellar energies. In a particular,  $S_{116}^{\text{g.s.}}(E) = 0.44 \pm 0.04$  and  $0.45 \pm 0.05 \text{ keV}\cdot\text{b}$  as well as  $S_{116}^{\text{exc.}}(E) = 9.89 \pm 1.01$  and  $9.20 \pm 0.94 \text{ keV}\cdot\text{b}$  are obtained for  $E = 0$  and  $25 \text{ keV}$ , respectively. And, the total astrophysical  $S$  factors  $S_{116}(E)$  are found to be  $10.34 \pm 1.06$  and  $9.65 \pm 0.98 \text{ keV}\cdot\text{b}$  for  $E = 0$  and  $25 \text{ keV}$ , respectively. One notes that our result for  $E = 0$  agrees with that of  $S_{116}(0) = 9.45 \pm 0.4 \text{ keV}\cdot\text{b}$  [8] and with the results of  $10.2$  and  $11.0 \text{ keV}\cdot\text{b}$  [10] obtained within the framework of the microscopic model for the effective V2 and MN potentials of the NN potential, respectively.

In Fig. 6, the results for the astrophysical  $S$  factors ( $S_{119}(E)$ ) for the nuclear-astrophysical  $^{19}\text{F}(p, \alpha)^{16}\text{O}$  reaction, obtained in the present work for corresponding six proton energies mention above, are displayed by open and full cycle points. They were obtained from the expressions (A1), (A10) and A(11) of Appendix with the fitted coefficients  $a_n(E)$  ( $0 \leq n \leq 2$ ) from Table 5 and the corresponding ANC  $C_{19\text{F}}^2$  values for  $^{16}\text{O} + t \rightarrow ^{19}\text{F}$  from Table 1. There, the uncertainty for each the energy  $E$  corresponds respectively to that of the  $C_{19\text{F}}^2$  ANC. Open and full cycle points in Fig. 6 correspond respectively to the  $C_{19\text{F}}^2$  values obtained in the present work from the analysis of the EXP-1978 data [26] for  $E = 237.5$ ;  $332.5$  and  $427.5 \text{ keV}$  and the EXP-2015 data [9] for  $E = 310.7$ ;  $367.7$  and  $461.7 \text{ keV}$ . The experimental data plotted in Fig. 6 by star points are taken from Refs. [9, 37]. As is seen from this figure, the open cycle data are in a reasonable agreement with those of Refs. [9, 37], whereas the full cycle data differ noticeably from them. This discrepancy is mainly the result of the fact that the corresponding  $C_{19\text{F}}^2$  values used in Eqs. (A10a) and (A10b) are underestimated by a factor of about 2 compared to those obtained from the analysis of the EXP-2015 [9]. Therefore, the present complex analysis performed on the basis of the asymptotic theory developed in [19] gives strong evidence that  $^{19}\text{F}(p, \alpha)^{16}\text{O}$  astrophysical  $S$  factors at the considered thermonuclear energies, which belong to the energy region considered in Refs. [9, 37], is dominant by the one-step triton transfer pole mechanism in which the three-body Coulomb dynamics in the main transfer mechanism is taken into account correctly.

On the other hand, the data for  $S_{119}(E)$  plotted in Fig. 6 by open cycles can be parametrized in the analytical form

$$S_{119}(E) = (31.09 \pm 1.08) - (39.44 \pm 2.53)E + (9.34 \pm 2.41)E^2, \quad (2)$$

in which  $S_{119}(E)$  in  $\text{MeV b}$  and  $E$  in  $\text{MeV}$ . Herein, the uncertainties in the coefficients of the polynomial expansion correspond to those of the fitted data within their errors. In Fig. 6, the solid curve corresponds to the calculated polynomial approximation of Eq. (2) for the

central values of its coefficients. While, the upper and lower dashed curves are the results of the calculation of Eq. (2) with the coefficients corresponding respectively to their upper and lower values. As seen from this figure, the polynomial approximation (2) reproduces reasonably also the absolute values of the data of [9]. Therefore, Eq. (2) can be used for calculation of  $S_{119}(E)$  in the nonresonant energy range, where the direct mechanism is dominant, including at  $E \leq 50$  keV. In particular,  $S_{119}(E)=31.09\pm 1.08$ ,  $30.11\pm 1.08$  and  $29.14\pm 1.09$  MeV b for  $E=0$ , 25 and 50 keV, respectively. They are significantly larger than both  $S_{119}(E)=8.76$ , 8.67 and 8.61 MeV b for  $E=0$ , 25 and 50 keV, respectively, derived in [27] from the DWBA analysis of the EXP-1978 data [26] and the corresponding values reported in NACRE [21] plotted in Fig. 6 by the dotted curve. The latter were derived from the nonresonant linear extrapolated formula used for the experimental  $S_{119}(E)$  data [38] from the fairly narrow energy range of  $E \sim 600$  keV (see the full triangle points in Fig. 6). One notes that the  $S_{119}(E)$  data of Ref. [38] are noticeably underestimated as a comparison with those of [9].

## VII. THERMONUCLEAR ${}^9\text{Be}(p, \gamma){}^{10}\text{B}$ AND ${}^{16}\text{O}(p, \gamma){}^{17}\text{F}$ REACTIONS RATES

The new values obtained for the total astrophysical  $S$  factors for the  ${}^9\text{Be}(p, \gamma){}^{10}\text{B}$  and  ${}^{16}\text{O}(p, \gamma){}^{17}\text{F}$  reactions were used to calculate the rates of these reactions as a function of stellar temperature within the range of  $10^{-3} \leq T_9 \leq 10$ , where  $T_9$  is a temperature in unit of  $10^9$  K. The Maxwellian-averaged reaction rates  $N_A \langle \sigma_{ij} v_{ij} \rangle$  are given by [1, 2]

$$N_A \langle \sigma_{ij} v_{ij} \rangle = N_A \left( \frac{8}{\pi \mu_{ij}} \right)^2 (k_B T)^{-3/2} \int_0^\infty S_{ij}(E) \exp[-E/k_B T - 2\pi \eta_{ij}] dE \quad (3)$$

as a function of the temperature  $T$ . Herein  $N_A$  is the Avogadro number;  $k_B$  is the Boltzmann constant;  $\mu_{ij}$  and  $\eta_{ij} = Z_i Z_j e^2 / \hbar v_{ij}$  are the reduced mass and the Coulomb parameter for the colliding ( $i$  and  $j$ ) particles, respectively, and  $v_{ij} = \sqrt{2E/\mu_{ij}}$ , where  $Z_k e$  is the charge of the particle  $k$ .

To calculate the  $N_A \langle \sigma_{116} v_{116} \rangle$  rate for the  ${}^{16}\text{O}(p, \gamma){}^{17}\text{F}$  reaction, the contributions of the resonant ( $E^*=3.104$  MeV with  $J^\pi=\frac{1}{2}^-$  and  $E^*=3.851$  MeV with  $J^\pi=\frac{5}{2}^-$ ) states of  ${}^{17}\text{F}$  to the total astrophysical  $S$  factor  $S_{116}(E)$  have been taken into account within the modified  $R$ -matrix method, similar to that as it is done for the  ${}^9\text{Be}(p, \gamma){}^{10}\text{B}$  reaction above. At this, we considered the transitions from the first and second resonant states mentioned above to the first excited and ground bound states of the residual  ${}^{17}\text{F}$  nucleus, respectively [22]. Both the transitions correspond to the dominant  $E1$  and  $M1$  ones. The values of the  $\gamma$ -widths corresponding to the first and second resonances as well as of the proton and total widths are taken from [39]. The direct component of  $S_{116}(E)$  is determined by the corresponding ANC values for  ${}^{16}\text{O} + p \rightarrow {}^{17}\text{F}$  derived in the present work. Besides, we calculate the reaction rate without taking into account the resonance contribution to the amplitude reaction. Both the method gave practically the same results for the  $N_A \langle \sigma_{116} v_{116} \rangle$  rate.

The resulting numerical values of the  ${}^9\text{Be}(p, \gamma){}^{10}\text{B}$  and  ${}^{16}\text{O}(p, \gamma){}^{17}\text{F}$  reaction rates in the temperature range  $0.01 \leq T_9 \leq 10$  K are presented in Table 4. Fig. 7(a) shows the ratios of the rates for the  ${}^9\text{Be}(p, \gamma){}^{10}\text{B}$  reaction calculated in the present work to those of Ref. [21] (the solid

curve) and [40] (the dashed line). Whereas, those for the  $^{16}\text{O}(p, \gamma)^{17}\text{F}$  reaction calculated in the present work to those of Ref. [21] (the solid curve) and [41] (the dashed line) are displayed in Fig. 7(b). The calculations show that, at temperatures  $T_9 \gtrsim 0.004$  K, the difference between the calculated rates recommended in the present work and those recommended in [21] and [40] is noticeable, whereas, it increases with decreasing the temperature (see the inserts in Fig. 7). One of the possible reasons of this discrepancy can apparently be associated with the model assumption used in [21, 40, 41], in particular, with the choice of the values of the spectroscopic factors for the  $^{10}\text{B}$  in the  $(^9\text{B} + p)$  configuration and the  $^{17}\text{F}$  in the  $(^{16}\text{O} + p)$  one, which really are strongly model dependent [8, 17] as noted above.

## VIII. CONCLUSION

Within the asymptotic theory proposed in [19] for the peripheral sub- and above-barrier charged-particle transfer  $A(x, y)B$  reaction, where  $x=(y + a)$ ,  $B=(A + a)$  and  $a$  is the transferred particle, the analysis is performed for the experimental angular distributions of the differential cross sections of the specific peripheral proton and triton transfer reactions at above- and sub-barrier projectile energies, respectively. It is demonstrated that the asymptotic theory gives an adequate description both of the angular distributions in the angular region of the main peaks of the angular distributions and of the absolute values of the specific ANC's (NVC's). New values and their uncertainties are obtained for the square of the ANC's for  $^9\text{Be} + p \rightarrow ^{10}\text{B}$ ,  $^{16}\text{O} + p \rightarrow ^{17}\text{F}$  and  $^{16}\text{O} + t \rightarrow ^{19}\text{F}$ . The accuracy of the “post”-approximation and the “post” form of the conventional DWBA is estimated for the ANC values for  $^9\text{Be} + p \rightarrow ^{10}\text{B}$  and  $^{16}\text{O} + p \rightarrow ^{17}\text{F}$  obtained by other authors in Refs. [24] and [17], respectively. The ANC values obtained in the present work were then applied for calculations of the astrophysical  $S$  factors for the radiative capture  $^9\text{Be}(p, \gamma)^{10}\text{B}$  and  $^{16}\text{O}(p, \gamma)^{17}\text{F}$  reactions at stellar energies as well as of the nuclear-astrophysical  $^{19}\text{F}(p, \alpha)^{16}\text{O}$  reaction at sub-barrier energies. New values and their uncertainties are obtained for the astrophysical  $S$  factors at thermonuclear energies. It is shown that the present analysis gives strong evidence that  $^{19}\text{F}(p, \alpha)^{16}\text{O}$  astrophysical  $S$  factors (or respective cross sections) at energies within the range of  $238 \lesssim E \lesssim 462$  keV is dominant by the one-step triton transfer pole mechanism in which the three-body Coulomb dynamics in the main transfer mechanism is taken into account in a correct manner. And, new values of the rates of  $^9\text{Be}(p, \gamma)^{10}\text{B}$  and  $^{16}\text{O}(p, \gamma)^{17}\text{F}$  reactions were obtained at stellar temperature within the range of  $10^{-3} \leq T_9 \leq 10$ , which show the noticeable difference (up to  $\sim 1.2$  and  $\sim 1.3$  times) with those recommended in [21, 40] and [21, 41], respectively.

## ACKNOWLEDGEMENT

The authors are deeply grateful to L.D. Blokhintsev for discussions and constructive suggestions and to S.V. Artemov for interest. This work has been supported in part by the Academy of Sciences of the Republic of Uzbekistan and by the Ministry of Education and Science of The Republic of Kazakhstan (grant No. AP05132062).

## APPENDIX: THE BASED FORMULES OF THE MODIFIED $R$ -MARTIX METHOD AND THE MODIFIED TWO-BODY POTENTIAL METHOD

Here we present only the idea and the main formulas for the astrophysical  $S$  factors of the modified  $R$ -method (see, for example, Ref. [33, 42] and references therein) and the MTBPM [34] specialized for the  ${}^9\text{Be}(p, \gamma){}^{10}\text{B}$  and  ${}^{16}\text{O}(p, \gamma){}^{17}\text{F}$  reactions, respectively, as well as the way of obtaining the  ${}^{19}\text{F}(p, \alpha){}^{16}\text{O}$  astrophysical  $S$  factors at thermonuclear energies, where the direct pole mechanism may be dominant. The orbital angular momentum of the proton capture is equal to 1 both for the ground and first three excited bound states of the residual  ${}^{10}\text{B}$  nucleus and for all the considered proton capture resonance states of  ${}^{10}\text{B}$  formed in the intermediate state.

The astrophysical  $S$  factor is determined by

$$S_{ij}(E) = Ee^{2\pi\eta}\sigma_{ij}(E), \quad (\text{A1})$$

where  $\sigma_{ij}(E)$  is the reaction cross section,  $E$  and  $\eta$  are the relative kinetic energy and the Coulomb parameter of the colliding particles  $i$  and  $j$ . In (A1), the indexes at the astrophysical  $S$  factor and the cross section denote mass numbers of the colliding particles.

According to [33, 42], within the framework of the modified  $R$ -matrix method, the total cross section for the  ${}^9\text{Be}(p, \gamma){}^{10}\text{B}$  reaction populating the ground ( ${}^{10}\text{B}_0$ ) and first three excited ( ${}^{10}\text{B}_f$ ) bound states of the residual  ${}^{10}\text{B}$  nucleus is given by

$$\sigma_{116}(E) = \sum_{f=0}^3 \sum_J \sigma_{J_{10}\text{B}_f J}(E). \quad (\text{A2})$$

Here  $J$  and  $J_{10}\text{B}_f$  are the total angular momentum of the colliding particles and the spin of the  $f$ th bound state in the  ${}^{10}\text{B}$  nucleus and

$$\sigma_{J_{10}\text{B}_f J}(E) = \frac{\pi}{k^2} \frac{2J+1}{8} \sum_{I l_i \lambda} |M_{J_{10}\text{B}_f J I l_i \lambda}(E)|, \quad (\text{A3})$$

where  $I$  and  $l_i$  are the channel spin and the relative orbital momentum of the  $p$ <sup>9</sup>Be-scattering, respectively,  $\lambda$  is the multipolarity order for the electromagnetic transition and  $k = \sqrt{2\mu_{p^9\text{Be}}E}/\hbar$  in which  $\mu_{p^9\text{Be}}$  is the reduced mass of  $p$  and  ${}^9\text{Be}$ . By using this case, one notes that there is misprint in the left-hand side of Eq. (5) in [33]. There, the expression  $\sigma_{J_i}(E)$  should be replaced by that of  $\sigma_{J_f}(E)$ . In Eq. (A3),  $M_{J_{10}\text{B}_f J I l_i \lambda}(E)$  is the amplitude of the electromagnetic ( $E\lambda$  and  $M\lambda$ ) transition, which is represented in the form

$$M_{J_{10}\text{B}_f J I l_i \lambda}(E) = M_{J_{10}\text{B}_f J I l_i \lambda}^{(R_{j_0}; (E\lambda, M\lambda))}(E) + M_{J_{10}\text{B}_f J I l_i \lambda}^{(\text{DC}; E\lambda)}(E) + M_{J_{10}\text{B}_f J I l_i \lambda}^{(\text{DC}; M\lambda)}(E), \quad (\text{A4})$$

where  $M_{J_{10}\text{B}_f J I l_i \lambda}^{(R_{j_0}; (E\lambda, M\lambda))}$  is the proton capture amplitude of the  $j_0$ th resonance state,  $M_{J_{10}\text{B}_f J I l_i \lambda}^{(\text{DC}; E\lambda)}$  and  $M_{J_{10}\text{B}_f J I l_i \lambda}^{(\text{DC}; M\lambda)}$  are the direct proton  $E\lambda$  and  $M\lambda$  capture amplitudes in the  $f$ th bound state

of  $^{10}\text{B}_f$ , respectively. In the single-level approximation, the  $M_{J_{10}\text{B}_f}^{(R_{j_0}; (E\lambda, M\lambda))}$  amplitude can be represented in the form [20, 42]

$$M_{J_{10}\text{B}_f}^{(R_{j_0}; (E\lambda, M\lambda))} = ie^{i(\sigma_{l_i}^{(c)} - \delta_{l_i}^{(\text{HS})})} \frac{[\Gamma_{Jl_i}^p(E)]^{1/2} [\Gamma_{J_{10}\text{B}_f}^{\gamma} J\lambda(E)]^{1/2}}{E - E_{R_{j_0}} + i\frac{\Gamma_J(E)}{2}}. \quad (\text{A5})$$

Here  $\sigma_{l_i}^{(c)}$  and  $\delta_{l_i}^{(\text{HS})}$  are the Coulomb and hard-sphere phase-shifts for the  $p^9\text{Be}$ -scattering;  $\Gamma_{Jl_i}^p(E)$  and  $\Gamma_{J_{10}\text{B}_f}^{\gamma} J\lambda(E)$  are the partial protonic and radiative  $\gamma$ -widths for the resonant decays  $^{10}\text{B}_{j_0} \rightarrow ^9\text{Be} + p$  and  $^{10}\text{B}_{j_0} \rightarrow ^{10}\text{B}_f + \gamma$ , respectively, and  $\Gamma_J(E)$  is the total ( $p$ ,  $\alpha$  and  $\gamma$ ) width. The energy dependence of the protonic and radiative  $\gamma$ -widths is given by the expressions

$$\Gamma_{Jl_i}^p(E) = \frac{2P_{l_i}(E)(\gamma_{Jl_i}^p)^2}{1 + (\gamma_{Jl_i}^p)^2 \left(\frac{dS_c}{dE}\right)_{E=E_{R_{j_0}}}} \quad (\text{A6a})$$

and

$$\Gamma_{J_{10}\text{B}_f}^{\gamma} J\lambda(E) = \frac{2k_{\gamma}^{2\lambda+1}(E)(\gamma_{J_{10}\text{B}_f}^{\gamma} J\lambda)^2}{1 + (\gamma_{Jl_i}^p)^2 \left(\frac{dS_c}{dE}\right)_{E=E_{j_0}}}, \quad (\text{A6b})$$

where  $k_{\gamma}$  is the photon momentum,  $P_{l_i}$  is the penetrability factor,  $S_c$  is the Thomas shift factor [43], and  $\gamma_{\dots}^p$  and  $\gamma_{\dots}^{\gamma}$  are the partial reduced protonic and radiative  $\gamma$ -ray widths, respectively. The reduced  $\gamma_{J_{10}\text{B}_f}^{\gamma} J\lambda$  width involves the internal ( $\gamma_{J_{10}\text{B}_f}^{\gamma} J\lambda(\text{int.})$ ) and external channel ( $\gamma_{J_{10}\text{B}_f}^{\gamma} J\lambda(\text{ext.})$ ) parts [20]. The external channel part is a complex number and contains the ANC for  $^9\text{Be} + p \rightarrow ^{10}\text{B}_f$  as a factor and the channel radius ( $r_{\text{ch}}$ ) as a free parameter. The observable partial protonic and radiative  $\gamma$ -widths are given by

$$\Gamma_{Jl_i}^p = |\Gamma_{Jl_i}^p(E_{R_{j_0}})|, \quad \Gamma_{J_{10}\text{B}_{j_0}}^{\gamma} J\lambda = |\Gamma_{J_{10}\text{B}_{j_0}}^{\gamma} J\lambda(E_{R_{j_0}})|. \quad (\text{A7})$$

One notes once more that, in [7], the contribution of the external part (so-called the proton-channel contribution) to the  $\Gamma_{J_{10}\text{B}_{j_0}}^{\gamma} J\lambda$  width was ignored, which really contains the ANC's for  $^9\text{Be} + p \rightarrow ^{10}\text{B}_f$ .

The explicit expressions for the direct capture amplitudes for the  $E\lambda$  and  $M\lambda$  transitions have rather cumbersome forms and, so, they are not presented here. Nevertheless, we note only that, in the long wavelength approximation, they contain the radial integral, which has the form as

$$I_{\lambda; Jl_i}(E) = C_{10\text{B}_f; J} \int_{r_{\text{ch}}}^{\infty} dr r^{\tilde{\lambda}} W_{-\eta_{10\text{B}_f}; 3/2}(2\kappa_{10\text{B}_f} r) (I_{l_i}(kr) - e^{i(\sigma_{l_i}^{(c)} - \delta_{l_i}^{(\text{HS})})} O_{l_i}(kr)), \quad (\text{A8})$$

where  $\tilde{\lambda} = \lambda$  and  $(\lambda-1)$  for the  $E1$  and  $M1$  transitions, respectively;  $W_{-\eta_{10\text{B}_f}; 3/2}(\dots)$  is the Whittaker function;  $\kappa_{10\text{B}_f} = \sqrt{2\mu_p^9\text{Be}\varepsilon_{10\text{B}_f}}/\hbar$  in which  $\varepsilon_{10\text{B}_f}$  is the binding energy of the  $f$ th bound state of  $^{10}\text{B}_f$  in the ( $^9\text{Be} + p$ ) channel, and  $I_{l_i}(kr)$  and  $O_{l_i}(kr)$  are the incoming and outgoing solutions of the radial Schrödinger equation.

As is seen from the expression (A8), the powers of the total direct capture amplitude and the channel radiative  $\gamma$ -width are determined by the ANC's for  ${}^9\text{Be} + p \rightarrow {}^{10}\text{B}_f$  ( $f=0-3$ ). Hence, introduction of information about the reliable “indirect measured” ANC's to the resonance and direct capture amplitudes makes it possible to reduce the uncertainty of the total  $S_{116}(E)$  astrophysical  $S$  factors calculated for the  ${}^9\text{Be}(p, \gamma){}^{10}\text{B}$  reaction in thermonuclear energy region to a minimum, as it is possible.

Within the framework of the MTBPM [34] (see, Ref. [8] also), the expression for the astrophysical  $S$  factors of the direct radiative capture  ${}^{16}\text{O}(p, \gamma){}^{17}\text{F}$  reaction populating the ground and first excited states of the residual  ${}^{17}\text{F}$  nucleus is presented in the form

$$S_{l_{17\text{F}_j}; 116}(E) = C_{17\text{F}_j; l_{17\text{F}_j}}^2 \mathcal{R}_{l_{17\text{F}_j}}(E; b_{17\text{F}_j}). \quad (\text{A9})$$

Here  $C_{17\text{F}_j; l_{17\text{F}_j}}$  is the ANC for  ${}^{16}\text{O} + p \rightarrow {}^{17}\text{F}_j$  ( $j=1$  and  $2$  for the ground and first excited states of  ${}^{17}\text{F}$ , respectively);  $b_{17\text{F}_j}$  is the single-particle ANC, which determines the amplitude of the “tail” of the radial component of the bound ( ${}^{16}\text{O} + p$ ) shell-model wave function of the  ${}^{17}\text{F}_j$  nucleus calculated using the Schrödinger equation with the adopted Woods-Saxon potential, and  $\mathcal{R}_{l_{17\text{F}_j}}(E; b_{17\text{F}_j}) = \sum_{\lambda} \tilde{S}_{l_{17\text{F}_j} \lambda; 116}(E; b_{17\text{F}_j}) / b_{17\text{F}_j}^2$  in which  $\tilde{S}_{l_{17\text{F}_j} \lambda; 116}(E; b_{17\text{F}_j})$  is the single-particle astrophysical  $S$  factor [21]. As shown in [8], the free parameter  $b_{17\text{F}_j}$  in turn depends strongly from the geometric parameters (the radius  $r_0$  and the diffuseness  $a$ ) of the adopted Woods-Saxon potential, i.e.,  $b_{17\text{F}_j} = b_{17\text{F}_j}(r_0, a)$ . In [8], the expression (A9) was used for determination of the “indirect measured” ANC's ( $C_{17\text{F}_j}$ ) by means of replacement of the astrophysical  $S$  factor in the left hand side of Eq. (A9) by their experimental data for each experimental point of the energy  $E$  [22]. This is connected by the fact that the reaction for each the fixed energy  $E$  is strongly peripheral, since the calculated values of the  $\mathcal{R}_{l_{17\text{F}_j}}(E; b_{17\text{F}_j})$  function as a function of the tree  $b_{17\text{F}_j}(r_0, a)$  parameter do not depend practically from variation of the free parameter. The results of the square of the ANC's obtained in Ref. [8] are also presented in Table 1. Nevertheless, the ANC's obtained in [8] for each the experimental point of the energy  $E$  have some spread associated with that of the data of Ref. [22] plotted in Fig. 5. On the other hand, the expression (A9) could also be used for calculation of  $S_{l_{17\text{F}_j} \lambda; 116}(E)$  if the “indirect measured” ANC's above are known from other independent precisely measured experimental data, e.g., from the experimental data for the peripheral  ${}^{16}\text{O}({}^3\text{He}, d){}^{17}\text{F}$  transfer proton reaction. This issue is considered in subsection B of Section VI.

We now show the way of applying the expression (1) for obtaining the total cross sections (respective the astrophysical  $S$  factor) of the sub-barrier  ${}^{19}\text{F}(p, \alpha){}^{16}\text{O}$  triton transfer reaction considered in Section VI. For this end, we split the limit of changing for the scattering angle ( $0 \leq \theta \leq 180$ ) in two intervals:  $0 \leq \theta \leq \theta_{\text{max}}$ , where good agreement between the experimental DCS's and the calculated ones occurs, and  $\theta_{\text{max}} < \theta \leq 180^\circ$ , where there is the noticeable discrepancy between the experimental DCS's and the calculated ones (see Fig. 3). Then, from Eq. (1) one has

$$\sigma_{119}(E) = \sigma_{<}(E) + \sigma_{>}(E), \quad (\text{A10a})$$

$$\sigma_{<}(E) = 2\pi C_{\alpha}^2 C_{19\text{F}_j}^2 \int_0^{\theta_{\text{max}}} d\theta \sin \theta \tilde{\sigma}_{r_0}(j_{19\text{F}}; E, \theta), \quad (\text{A10b})$$

$$\sigma_{>}(E) = 2\pi \int_{\theta_{\max}}^{180} d\theta \sin \theta \frac{d\sigma}{d\Omega}, \quad (\text{A10c})$$

where  $j_{19\text{F}} = 1/2$ ,  $E = E_i$ ,  $r_0 = 1.25$  fm, and the  $C_\alpha^2$  and  $C_{19\text{F}_j}^2$  ANC's are known. For each considered fixed proton projectile energy, the integral in the right-hand side of Eq. (A10b) can be taken numerically using the calculated  $\tilde{\sigma}_{r_0}(j_{19\text{F}}; E, \theta)$  function and the corresponding  $C_{19\text{F}_j}^2$  given in Table 1. Due to the fact that the experimental angular distributions of the  $^{19}\text{F}(p, \alpha)^{16}\text{O}$  reaction plotted in Fig. 3(a)–(f) monotonic decrease (including for  $\theta > \theta_{\max}$ ), similarly as it is done in Ref. [44], the Legendre polynomial expansion

$$\left( \frac{d\sigma}{d\Omega} \right)_{\theta > \theta_{\max}} = \sum_{n=0}^2 a_n(E) P_n(\cos \theta) \quad (\text{A11})$$

for the integrand function of the integral (A10c) is applied for reproducing the corresponding experimental DCS's in the angular range of  $\theta > \theta_{\max}$ . The values of the fitted  $a_n(E)$  coefficients of the expression (A11) providing well description of the experimental data in the corresponding angular range are given in Table 2. They can be used for calculating of the integral (A10c). The results of calculations of  $(d\sigma/d\Omega)_{\theta > \theta_{\max}}$  are displayed in Fig. 3 by the dotted curves. Thus, Eqs. (A10)–(A11) allow us to calculate the total cross sections (respective the astrophysical  $S$  factors) for the  $^{19}\text{F}(p, \alpha)^{16}\text{O}$  reaction for each fixed center-of-mass projectile energy from the EXP-1978 and EXP-2015 data.



## References

- [1] W.A. Fowler, Rev. Mod. Phys. **56**, 149 (1984).
- [2] C. Rolfs and W.S. Rodney, *Cauldrons in the Cosmos*,(University of Chicago Press,Chicago and London 1988).
- [3] E.G. Adelberger, A.Garcia, R. G. Hamish Robertson, K.A. Snover, A.B.Balantekin, K. Heeger, M. J, Ramsey-Musolf, D. Bemmerer, A. Junghans, C.A. Bertulani, J.-W. Chen, H. Costantini, P. Prati, M. Couder, E. Uberseder, M. Wiescher, R. Cyburt, B. Davids, S. J. Freedman, M. Gai, D. Gazit, L. Gialanella, G. Imbriani, U. Greife, M. Hass, W.C. Haxton, T. Itahashi, K. Kubodera, K. Langanke, D. Leitner, M. Leitner, P. Vetter, L. Winslow, L.E. Marcucci, T. Motobayashi, A.M. Mukhamedzhanov, R.E. Tribble, Konneth M. Nollett, F.M. Nunes, T.-S. Park, P.D. Parker, R. Schiavilla, E.C. Simpson, C. Spitaleri, F. Strieder, H.-P. Trautvetter, K. Suemmerer, S. Typel, Rev. Mod. Phys. **83**, 195 (2011).
- [4] L. D. Blokhintsev, R. Yarmukhamedov, S.V. Artemov, I. Boztosun, S.B. Igamov, Q.I. Tursunmakhtov, and M.K. Ubaydullaeva, Uzb. J. Phys. **12**, 217 (2010).
- [5] R. Yarmukhamedov, and Q.I. Tursunmahatov, *The Universe Evolution: Astrophysical and nuclear aspects. Edit. I. Strakovsky and L. D. Blokhintsev*. (New York, NOVA publishers, 2013), pp.219–270.
- [6] R.E. Tribble, C.A. Bertulani, M. La Cognata, A.M. Mukhamedzhanov, and C. Spitaleri, Rep. Prog. Phys. **77**, 901 (2014).
- [7] A. Sattarov, A.M. Mukhamedzhanov, A. Azhari, C.A. Gagliardi, L. Trache, and R.E. Tribble, Phys. Rev. C **60**, 035801 (1999).
- [8] S.V. Artemov, S.B. Igamov, Q.I. Tursunmakhatov, and R. Yamukhamedov, Bull. RAN. Ser. Phys. **73**, 176 (2009) [Izv. RAN. Ser. Fiz. **73**, 165 (2009)].
- [9] I. Lombardo, D. Dell’Aquila, A.Di Leva, I. Indelicato, M. La Cognata, M. La Commara, A. Ordine, V. Rigato, M. Romoli, F. Rosalo, G. Spadaccini, C. Spitareli, A. Tumino, and M. Viliance, Phys. Lett. **B778**, 178 (2015).
- [10] D. Baye, P. Descouvemont, and M. Hesse, Phys. Rev. **C58** (1998) 545.
- [11] E.A. Wulf, M.A. Godwin, J.F. Guillemette, C.M. Laymon, R.M. Prier, B.J. Rice, V. Spraker, D.R. Tilley, H.R. Weller, Phys. Rev. **C58**, (1998) 517.
- [12] L.D. Blokhintsev, A.S. Kadyrov, A.M. Mukhamedzhanov, D.A. Savin, Phys. Rev. C **98**, 064610 (2018).
- [13] H. Herndl, H. Abele, G. Staudt, B. Bach, K. Grün, H. Scsribany, H. Oberhummer, G. Raimann, Phys. Rev. **C44**, R952 (1991).

- [14] F.E. Cecil, D. Ferg, H. Liu, J.C. J.C. Scorby, J.M. McNeil, and P.D. Kunz, Nucl. Phys. **A539**, 75 (1992).
- [15] D. Zahnow, C Angulo, M. Junker, C. Rofs, S. Schimidt, W.H. Schulte, and E. Somorjai, Nucl. Phys. **A589**, 95 (1995).
- [16] C. Rofs, Nucl. Phys. **A217**, 29 (1973).
- [17] A. M. Mukhamedzhanov, H. L. Clark, C. A. Gagliardi, Y.-W. Lui, L. Thache, R. E. Tribble, H. M. Xu, X. G. Zhou, V. Burjan, J. Cejpek, V. Kroha, and F. Carstoui, Phys. Rev. **C56**, 1302 (1997).
- [18] Sh.S. Kajumov, A.M. Mukhamedzhanov, R. Yarmukhamedov, and I. Borbely, Z. Phys. A **336**. 297 (1990).
- [19] R. Yarmukhamedov and K.I. Tursunmakhatov, submitted to Phys. Rev. C, 2019.
- [20] R.J. Holt, H.E. Jackson, R.M. Laszewski, J.E. Monahan, and J.R. Spechi, Phys. Rev. **C18**, 1962 (1978).
- [21] C. Angulo, M. Arnould, M. Rayet, P. Descouvemont, D. Baye, C. Leclercq-Willain, A. Coc, S. Barhoumi, P. Aguer, C. Rofs, R. Kunz, J. W. Hammer, A. Mayer, T. Paradellis, S. Kossionides, C. Chronidou, K. Spyrou, S. Degl'Innocenti, G. Fiorentini, B. Ricci, S. Zavatarelli, C. Providencia, H. Wolters, J. Soares, C. Grama, J. Rahighi, A. Shotter, M. L. Rachti, Nucl. Phys. **A656**, 3 (1999).
- [22] R. Morlock, R. Kunz, A. Mayer, M. Jaeger, A. Müller, J.M. Hummer, P. Mohr, H. Oberhummer, G. Staudt, and V. Kölle, Phys. Rev. Lett. **79**, 3837 (1997).
- [23] C.A. Gagliardi, R.E. Tribble, A. Azhari, H. L. Clark, Y.-W. Lui, A. M. Mukhamedzhanov, A. Sattarov, L. Thache, V. Burjan, J. Cejpek, V. Kroha, Š. Piskov, and J. Vincour, Phys. Rev. C **59**, 1149 (1999).
- [24] S. V. Artemov, I. R. Gulamov, E. A. Zapparov, I. Yu. Zotov, and G. K. Nie, Yad. Fiz. **59**, 454 (1996)[Phys. At. Nucl. **59**, 428 (1996)].
- [25] R. Yarmukhamedov and D. Baye, Phys. Rev. **C84**, 24603 (2011).
- [26] H. Lorenz-Wirzha, Ph.D. thesis, Universität, Münster, 1978.
- [27] H. Herndl, H. Abele, G. Staudt, B. Bach, K. Grün, H. Scsribany, H. Oberhummer, G. Raimann, Phys. Rev. C **44**, R952 (1991).
- [28] L.D. Blokhintsev, I. Borbely, E.I. Dolinskii, Phys. Part. Nucl. **8**, 485 (1977).
- [29] R. Yarmukhamedov and L. D. Blokhintsev, Phys. At. Nucl. **81**, 616 (2018).
- [30] G. R. Plattner, R. D. Viollier, D. Trautmann, K. Alder, Nucl. Phys. A **206**, 513 (1973).

- [31] S.V. Artemov, A.B. Bajajin, S.B. Igamov, G.K. Nie, and R. Yamukhamedov, *Yad. Fiz.* **71**, 998 (2008)[*Phys. At. Nucl.* **71**, 1025 (2008)].
- [32] A.M. Mukhamedzhanov, R.E. Tribble, and N.K. Timofeyuk, *Phys. Rev. C* **51**, 3472 (1995).
- [33] S. V. Artemov, S. B. Igamov, Q. I. Tursunmakhatov, and R. Yarmukhamedov, *Phys. Atom. Nucl.* **75**, 291 (2012).
- [34] S. B. Igamov, and R. Yarmukhamedov, *Nucl. Phys. A* **781**, 247 (2007).
- [35] F. Ajzenberg-Selove, *Nucl. Phys. A* **490**, 1 (1988).
- [36] W. Auwärter and V. Mayer, *Nucl. Phys. A* **242**, 129 (1975).
- [37] M. La Cognata, C. Palmirini, C. Spitareli, I. Indelicato, A.M. Mukhamedzhanov, I. Lombardo, and O. Trippella, *Astron. J.* **805**, 128 (2015).
- [38] A. Isoya, H. Ohmura, and T. Momota, *Nucl. Phys.* **7**, 116, (1958).
- [39] R.B. Firestone, *Table of Isotopes CD-ROM, Info nucl A=1–20* (Version 1.0, March 1996), p. 158.
- [40] Y. Xu, K. Takahashi, S. Goriely, M. Arnould, M. Ohta, and H. Utsunomiya, *Nucl. Phys. A* **918**, 61 (2013).
- [41] C. Iliadis, C. Angulo, P. Discouvemont, M. Lugaro, and P. Mohr, *Phys. Rev. C* **77**, 045802 (2008).
- [42] F.C. Barker and T. Kajino, *Aust. J. Phys.* **44**, 369 (1991).
- [43] A.M. Lane and R.G. Thomas, *Rev. Mod. Phys.* **30**, 257 (1957).
- [44] G. Raimann, B. Bach, K. Grün, H. Herndl, H. Oberhummer, S. Engstler, C. Rolfs, H. Abele, R. Neu, and G. Staudt, *Phys. Lett.* **B249**, 191 (1990).

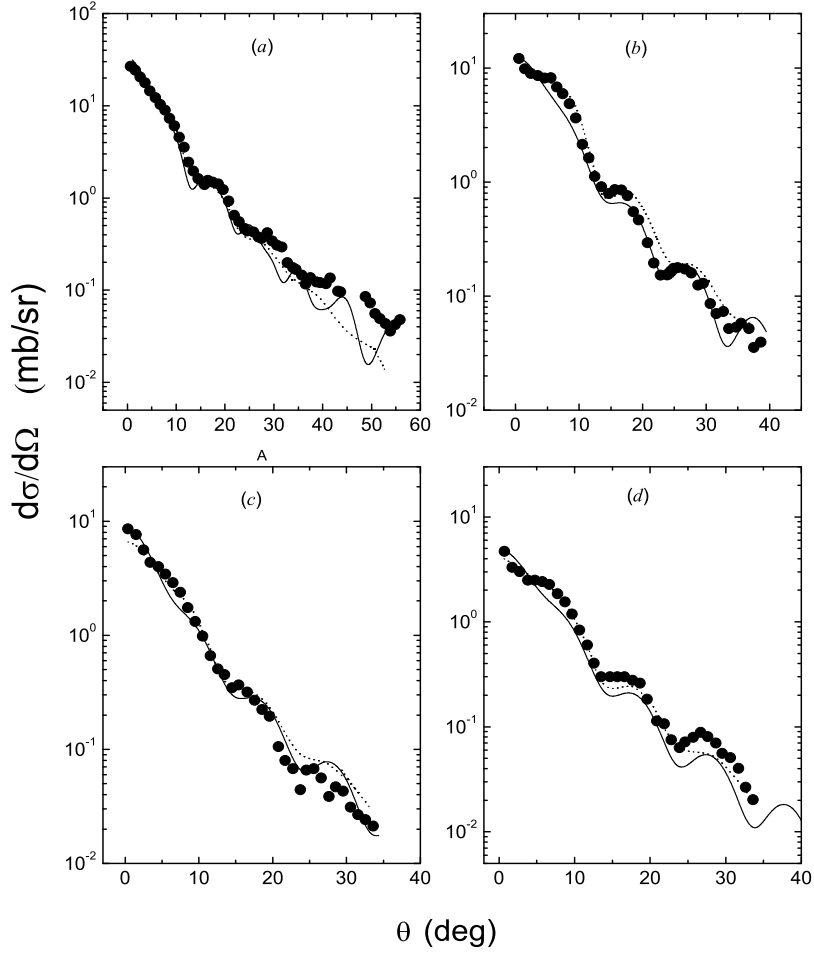


Figure 1: The differential cross sections for the  ${}^9\text{Be}({}^{10}\text{B}, {}^9\text{Be}){}^{10}\text{B}$  reaction at  $E_{10\text{B}} = 100$  MeV. The points are the experimental data taken from [17]. The solid and dashed lines are the results of the present work and the DWBA calculations of [17], respectively, for the ground (a), first (for  $E^* = 0.718$  MeV)(b), second (for  $E^* = 1.740$  MeV) (c) and third (for  $E^* = 2.154$  MeV) (d) excited states of the residual nucleus  ${}^{10}\text{B}$ .

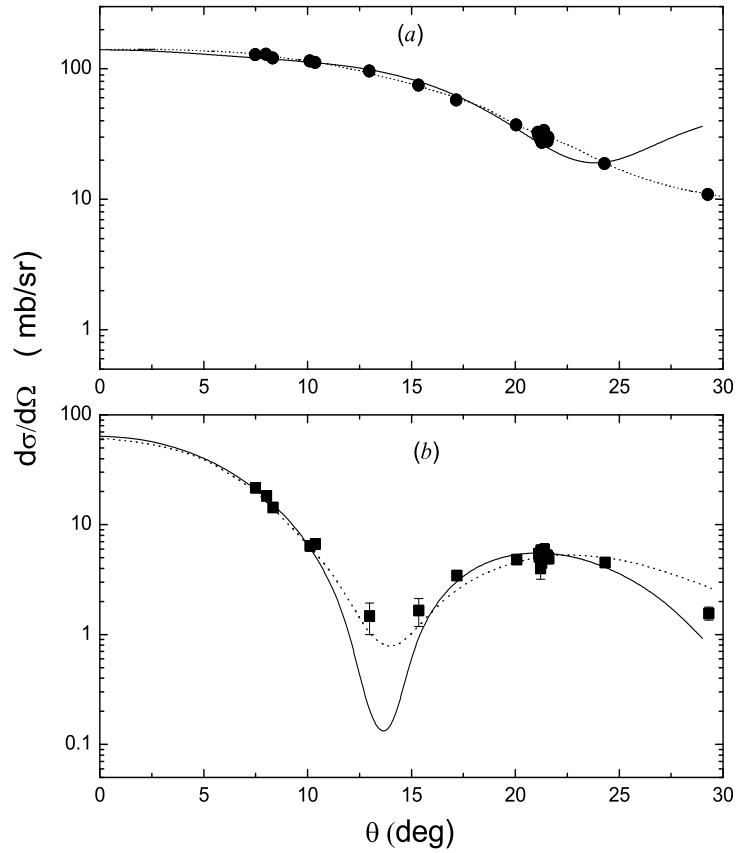


Figure 2: The differential cross sections for the  $^{16}\text{O}(^3\text{He}, d)^{17}\text{F}$  reaction corresponding to the ground (a) and first excited (0.429 MeV)(b) states of  $^{17}\text{F}$  at  $E_{^3\text{He}} = 29.75$  MeV. The solid and dashed curves are the results of the present work and those of Ref. [23] derived in the “post” form of the modified DWBA. The experimental data are taken from Refs. [23].

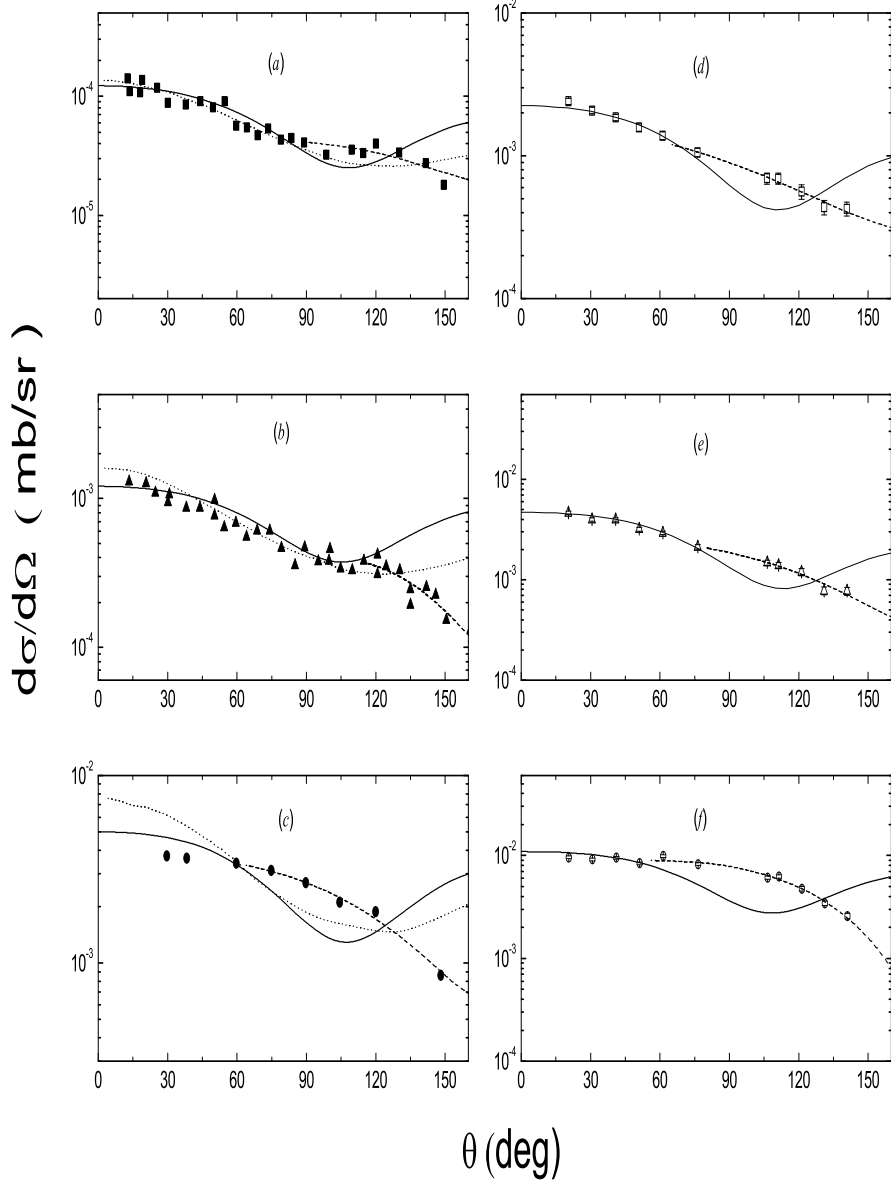


Figure 3: The differential cross sections for the  $^{19}\text{F}(p, \alpha)^{16}\text{O}$  reaction at  $E_p = 450$  (a), 350 (b) and 250 keV (c) (the left side) as well as  $E_p = 327$  (d), 387 (e) and 486 keV (f) (the right side). The solid and dotted curves are the results of the present work, whereas the dashed lines are the results of Ref. [27] derived in the zero-range of the “post”-approximation of DWBA. The dotted curves are presented our result obtained by means of the polynomial fit (see Eq. (A11) in Appendix and Table 5). The experimental data are taken from Refs. [26] (the EXP-1978:(a), (b) and (c), see [27] too) and [9] (the EXP-2015:(d), (e) and (f)).

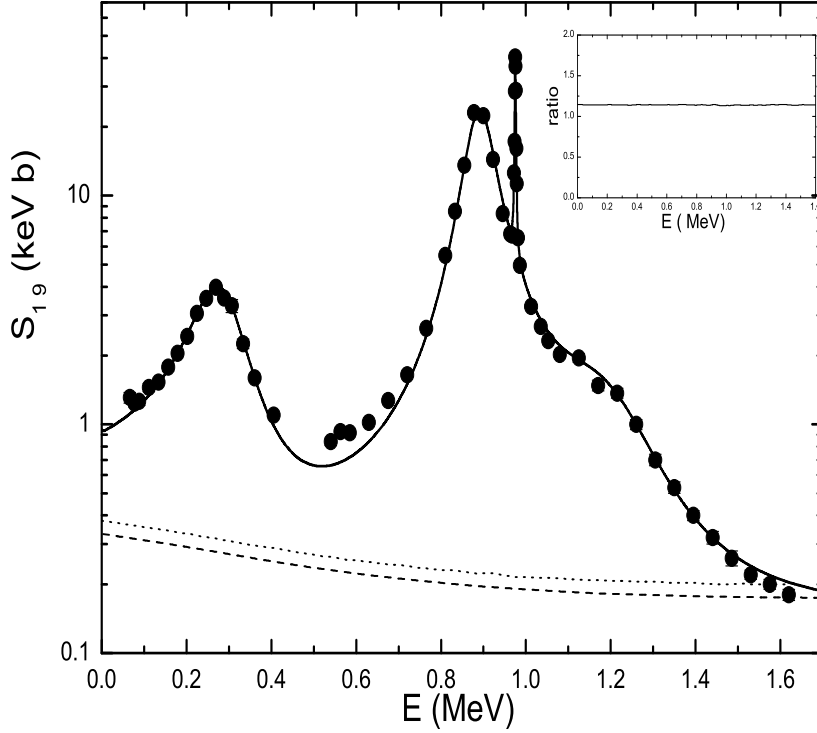


Figure 4: The total astrophysical  $S$  factor for the  ${}^9\text{Be}(p, \gamma){}^{10}\text{B}$  reaction. The points are the experimental data from [15]. The solid and dashed lines are the calculated results of the present work for the total and direct radiative capture, respectively. The curve in the insert is the ratio of the direct component of  $S_{19}(E)$  of Ref. [7] to that of the present work.

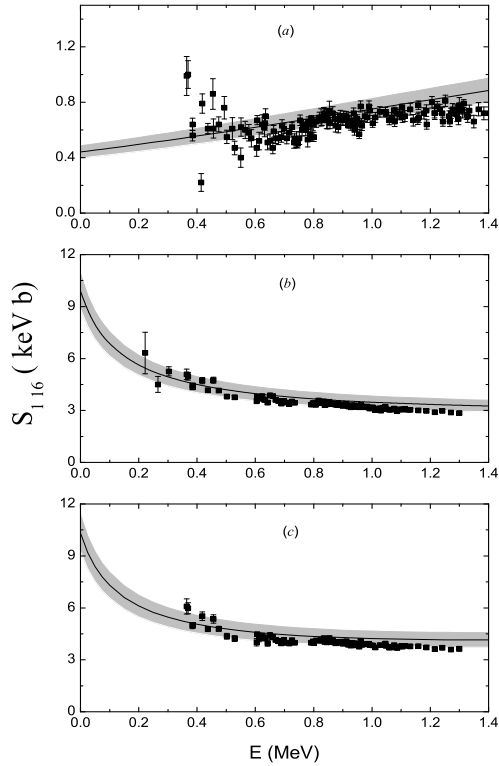


Figure 5: The astrophysical  $S$  factors for the direct radiative capture  $^{16}\text{O}(p, \gamma)^{17}\text{F}$  reaction. The curves of (a) and (b) correspond to the ground and first excited (0.495 MeV) states of the residual  $^{17}\text{F}$  nucleus, respectively, whereas that of (c) corresponds to their sum  $^{17}\text{F}$  (g.s. + 0.495 MeV). The solid and the band are the results of the present work, whereas the dashed line is the result of Ref. [8]. The experimental data are from [22].



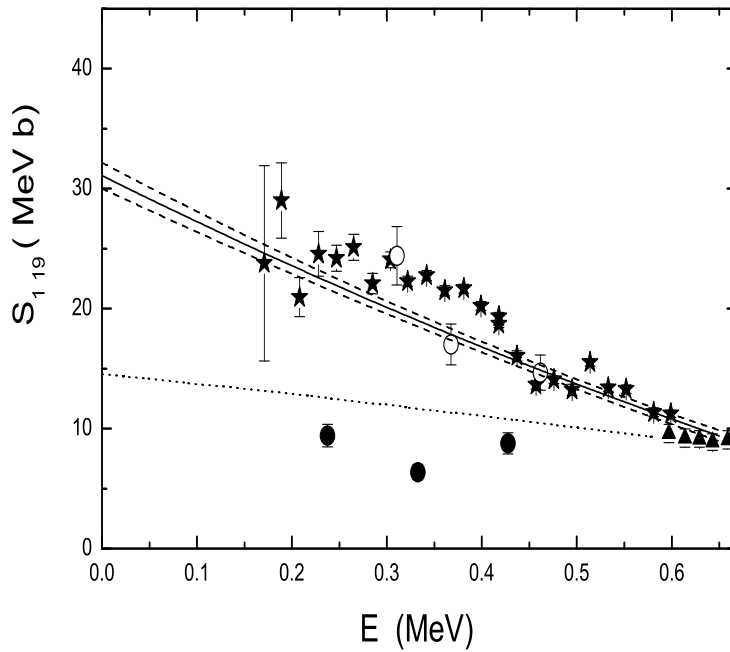


Figure 6: The astrophysical  $S$  factors for the direct radiative capture  $^{19}\text{F}(p, \alpha)^{16}\text{O}$  reaction: open and full circle points are our result for the direct  $S_{1,19}(E)$  astrophysical  $S$  factor obtained from the analysis of the EXP-1978 [26, 27] and EXP-2015 [9] data; The experimental star points are taken from Refs [9, 37] (stars points) and [38] (full triangle points). The solid curve corresponds to the polynomial fitting. The lower dotted curve is the results of Ref. [21] obtained from the linear extrapolated formula used for the experimental  $S_{1,19}(E)$  data of [38].

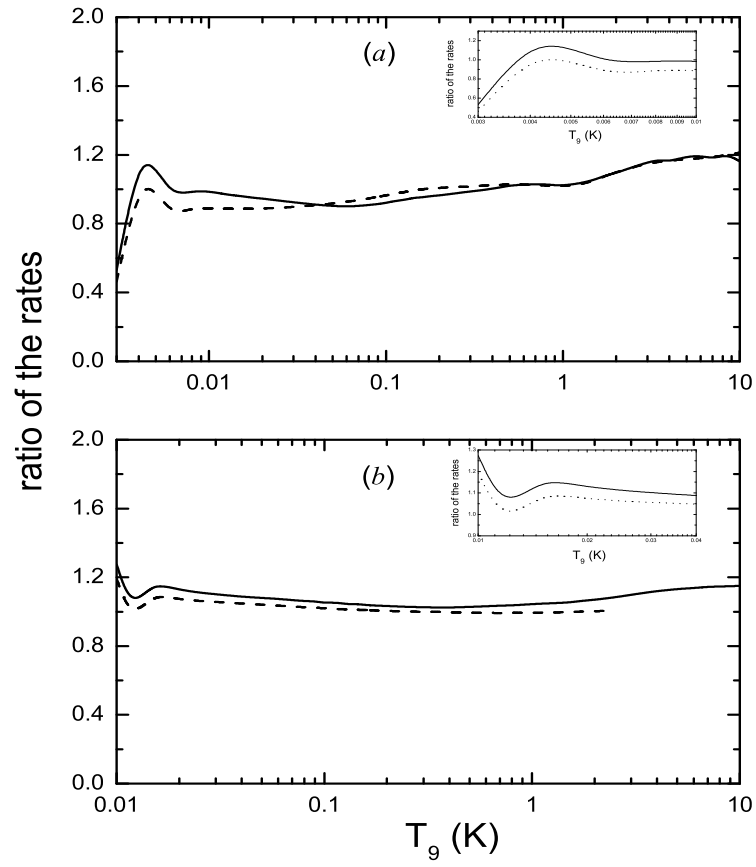


Figure 7: The ratios of the rates for the radiative capture  ${}^9\text{Be}(p, \gamma){}^{10}\text{B}$  (a) and  ${}^{16}\text{O}(p, \gamma){}^{17}\text{F}$  (b) reactions. Description is given in the text.

Table 1: Reaction, energy  $E_x$ , set of the optical potentials (set), virtual decay  $B \rightarrow A + a$ , orbital and total angular momentums ( $l_B, j_B$ ), square modulus of the nuclear vertex constant  $|G_B|^2$  ( $G_B = G_{Aa;l_B j_B}$ ) for the virtual decay  $B \rightarrow A + a$  and the corresponding ANC  $C_B^2$  ( $C_B = C_{Aa;l_B j_B}$ )  $A + a \rightarrow B$ . Figures in brackets are experimental and theoretical uncertainty, respectively, whereas those in square brackets are weighed mean derived from the ANC's (NVC's) values for the sets 1 and 2.

$A(x, y)B$	$E_x$ , MeV	set	$B \rightarrow A + a$	$l_B, j_B$	$ G_B ^2$ , fm	$C_B^2$ , fm <sup>-1</sup>
1	2	3	4	5	6	7
<sup>9</sup> Be( <sup>10</sup> B, <sup>9</sup> Be) <sup>10</sup> B <sub>0</sub>	100 [17]	1	<sup>10</sup> B <sub>0</sub> → <sup>9</sup> Be + p	1, 3/2	0.72(±0.06;±0.02)	4.22(±0.33;±0.10)
					0.72 ±0.06	4.22±0.35
		2			0.84±0.07 [17]	4.91±0.39 [17]
					0.77(±0.06;±0.02)	4.49(±0.37;±0.11)
					0.77 ±0.07	4.49±0.39
1+2	0.92±0.07 [17]	5.35±0.42 [17]				
					[0.75(±0.04;±0.02)]	[4.35(±0.24;±0.14)]
					[0.75±0.05]	[4.35±0.28]
					[0.87±0.08] [17]	[5.06±0.46] [17]
<sup>9</sup> Be( <sup>3</sup> He, d) <sup>10</sup> B <sub>0</sub>	22.3–32.5 [24]				0.63–0.73 [24]	3.67–4.20 [24]
<sup>9</sup> Be( <sup>10</sup> B, <sup>9</sup> Be) <sup>10</sup> B <sub>1</sub>	100 [17]	1	<sup>10</sup> B <sub>1</sub> → <sup>9</sup> Be + p	1, 1/2	0.22(±0.02;±0.01)	1.31(±0.10;±0.03)
					0.22 ±0.02	1.31±0.11
		2			0.21±0.03 [17]	1.23±0.17 [17]
					0.25(±0.02;±0.01)	1.47(±0.17;±0.03)
					0.25 ±0.02	1.47±0.17
1+2	0.23±0.03 [17]	1.34±0.19 [17]				
					[0.23(±0.02;±0.01)]	[1.33(±0.09;±0.03)]
					[0.23±0.02]	[1.33±0.10]
					[0.22±0.04] [17]	[1.27±0.21] [17]
<sup>9</sup> Be( <sup>3</sup> He, d) <sup>10</sup> B <sub>1</sub>	22.3–32.5 [24]	1		1, 3/2	0.62–0.69 [24]	3.16–4.02 [24]
					0.60(±0.05;±0.01)	3.53(±0.27;±0.09)
		0.60 ±0.05			3.53±0.29	
		2			0.57±0.05 [17]	3.33±0.29 [17]
					0.68(±0.05;±0.02)	3.98(±0.31;±0.09)
0.68 ±0.06	3.98±0.32					
1+2	0.23±0.05 [17]	3.63±0.32 [17]				
					[0.64(±0.04;±0.04)]	[3.74(±0.22;±0.23)]
					[0.64±0.05]	[3.74±0.32]
					[0.59±0.07] [17]	[3.43±0.42] [17]
<sup>9</sup> Be( <sup>3</sup> He, d) <sup>10</sup> B <sub>1</sub>	22.3–32.5 [24]				0.37–0.42 [24]	2.16–2.45 [24]
<sup>9</sup> Be( <sup>10</sup> B, <sup>9</sup> Be) <sup>10</sup> B <sub>2</sub>	100 [17]	1	<sup>10</sup> B <sub>2</sub> → <sup>9</sup> Be + p	1, 3/2	0.58(±0.04;±0.01)	3.39(±0.26;±0.08)
					0.58 ±0.05	3.39±0.27
		2			0.72±0.08 [17]	4.22±0.44 [17]
					0.66(±0.05;±0.02)	3.88(±0.30;±0.10)
					0.77 ±0.05	3.88±0.32
1+2	0.79±0.08 [17]	4.60±0.48 [17]				
					[0.61(±0.04;±0.02)]	[3.60(±0.24;±0.24)]
					[0.61±0.06]	[3.60±0.34]
					[0.74±0.09] [17]	[4.35±0.59] [17]
<sup>9</sup> Be( <sup>3</sup> He, d) <sup>10</sup> B <sub>2</sub>	32.5 [24]				1.25±0.14 [24]	7.29±0.82 [24]

Table 2: continuation of Table 1

1	2	3	4	5	6	7			
${}^9\text{Be}({}^{10}\text{B}, {}^9\text{Be}){}^{10}\text{B}_3$	100 [17]	1	${}^{10}\text{B}_3 \rightarrow {}^9\text{Be} + p$	1, 1/2	0.055( $\pm 0.004$ ; $\pm 0.001$ )	0.32( $\pm 0.03$ ; $\pm 0.01$ )			
					0.055 $\pm 0.004$	0.32 $\pm 0.03$			
		2		0.048 $\pm 0.009$ [17]	0.28 $\pm 0.05$ [17]				
				0.046( $\pm 0.004$ ; $\pm 0.002$ )	0.27( $\pm 0.02$ ; $\pm 0.01$ )				
				0.046 $\pm 0.005$	0.27 $\pm 0.03$				
		1+2		0.0513 $\pm 0.0085$ [17]	0.30 $\pm 0.05$ [17]				
				[0.055( $\pm 0.003$ ; $\pm 0.005$ )]	[0.32( $\pm 0.02$ ; $\pm 0.03$ )]				
		1		1, 3/2	[0.055 $\pm 0.005$ ]	[0.32 $\pm 0.03$ ]			
					[0.050 $\pm 0.010$ ] [17]	[0.29 $\pm 0.06$ ] [17]			
		2		0.155( $\pm 0.012$ ; $\pm 0.004$ )	0.91( $\pm 0.07$ ; $\pm 0.02$ )				
0.155 $\pm 0.012$	0.91 $\pm 0.07$								
0.14 $\pm 0.02$ [17]	0.80 $\pm 0.10$ [17]								
1+2	0.13( $\pm 0.01$ ; $\pm 0.01$ )	0.76( $\pm 0.07$ ; $\pm 0.04$ )							
	0.13 $\pm 0.01$	0.76 $\pm 0.08$							
	0.15 $\pm 0.02$ [17]	0.87 $\pm 0.11$ [17]							
${}^9\text{Be}({}^3\text{He}, d){}^{10}\text{B}_3$ ${}^{16}\text{O}({}^3\text{He}, d){}^{17}\text{F}_0$	32.5 [24] 29.75 [23]	1	${}^{17}\text{F} \rightarrow {}^{16}\text{O} + p$	2, 5/2	[0.15( $\pm 0.01$ ; $\pm 0.01$ )]	[0.89( $\pm 0.06$ ; $\pm 0.08$ )]			
					[0.15 $\pm 0.02$ ]	[0.89 $\pm 0.10$ ]			
		2		[0.14 $\pm 0.02$ ] [17]	[0.82 $\pm 0.12$ ] [17]				
				0.26 $\pm 0.03$ [24]	1.52 $\pm 0.17$ [24]				
				0.179( $\pm 0.018$ ; $\pm 0.009$ )	1.14( $\pm 0.12$ ; $\pm 0.06$ )				
		1+2		0.179 $\pm 0.020$	1.14 $\pm 0.13$				
				0.16 [23]	1.0 [23]				
				0.206( $\pm 0.021$ ; $\pm 0.010$ )	1.31( $\pm 0.14$ ; $\pm 0.07$ )				
		18;34 [24]		0.206 $\pm 0.024$	1.31 $\pm 0.15$				
				0.18 [23]	1.10 [23]				
[0.190( $\pm 0.014$ ; $\pm 0.013$ )]	[1.21( $\pm 0.09$ ; $\pm 0.08$ )]								
${}^{16}\text{O}(p, \gamma){}^{17}\text{F}_0$ The $p$ - ${}^{16}\text{O}$ -scattering: the phase-shifts analysis	29.75 [23]	1	${}^{17}\text{F} \rightarrow {}^{16}\text{O} + p$	0, 1/2	[0.190 $\pm 0.019$ ]	[1.21 $\pm 0.12$ ]			
					[0.170 $\pm 0.016$ ] [23]	[1.08 $\pm 0.10$ ] [23]			
		2		0.16 [24]	1.02 [24]				
				0.17 $\pm 0.02$ [8]	1.09 $\pm 0.11$ [8]				
				0.12 <sup>a</sup> [12]	0.77 <sup>a</sup> [12]				
		1+2		0.37 <sup>b</sup> [12]	5.48 <sup>b</sup> [12]				
				0.17 <sup>c</sup> [25]	1.09 <sup>c</sup> [25]				
				916( $\pm 96$ ; $\pm 46$ )	5840( $\pm 611$ ; $\pm 292$ )				
		${}^{16}\text{O}(p, \gamma){}^{17}\text{F}_1$ The $p$ - ${}^{16}\text{O}$ -scattering: the phase-shifts analysis		18; 34 [24]	1	${}^{17}\text{F} \rightarrow {}^{16}\text{O} + p$	0, 1/2	916 $\pm 106$	5840 $\pm 667$
								939 [23]	5980 [23]
2	1053( $\pm 110$ ; $\pm 53$ )		6713( $\pm 703$ ; $\pm 335$ )						
	1053 $\pm 122$		6713 $\pm 779$						
	1099 [23]		7000 [23]						
1+2	[975( $\pm 72$ ; $\pm 68$ )]		[6216( $\pm 461$ ; $\pm 432$ )]						
	[975 $\pm 99$ ]		[6216 $\pm 632$ ]						
	[1019 $\pm 107$ ] [23]		[6490 $\pm 680$ ] [23]						
840; 819 [24]	840; 819 [24]		5355; 5122 [24]						
	893 $\pm 35$ [8]		5700 $\pm 225$ [8]						
	1629 <sup>a</sup> [12]	10384 <sup>a</sup> [12]							
	1245 <sup>b</sup> [12]	7939 <sup>b</sup> [12]							
	893 <sup>c</sup> [25]	5700 <sup>c</sup> [25]							

Table 3: continuation of Table 1

1	2	3	4	5	6	7
$^{19}\text{F}(p, \alpha)^{16}\text{O}$	0.250 [26]		$^{19}\text{F} \rightarrow ^{16}\text{O} + t$	0, 1/2	13.5( $\pm 2.1$ ; $\pm 0.7$ )	618.1( $\pm 95.2$ ; $\pm 30.9$ )
EXP-1978	0.350				13.2( $\pm 1.4$ ; $\pm 0.7$ )	605.0( $\pm 63.4$ ; $\pm 30.3$ )
	0.450				11.9( $\pm 1.3$ ; $\pm 0.6$ )	544.8( $\pm 60.6$ ; $\pm 27.2$ )
weighed mean					12.7( $\pm 0.9$ ; $\pm 0.5$ )	583.5( $\pm 39.8$ ; $\pm 23.3$ )
					12.7 $\pm 1.0$	583.5 $\pm 46.1$
EXP-2015	0.327 [9]				28.1( $\pm 2.7$ ; $\pm 1.4$ )	1290.3( $\pm 124.0$ ; $\pm 64.3$ )
	0.387				29.2( $\pm 3.2$ ; $\pm 1.5$ )	1341.3( $\pm 144.7$ ; $\pm 66.6$ )
	0.486				27.2( $\pm 2.9$ ; $\pm 1.4$ )	1248.1( $\pm 134.6$ ; $\pm 62.5$ )
weighed mean					28.1( $\pm 1.7$ ; $\pm 0.8$ )	1291.1( $\pm 77.2$ ; $\pm 37.2$ )
					28.1 $\pm 1.9$	1291.1 $\pm 85.7$

<sup>a</sup>The effective-range function (RRF) method.

<sup>b</sup>The  $\Delta$  method.

<sup>c</sup>The effective-range expansion method for the  $p^{16}\text{O}$ -scattering function.

Table 4: The values of the fitted coefficients  $a_n(E)x10^4$  of the expression (A11) of Appendix for different center-of-mass energies  $E$ .  $E$  in keV and  $a_n(E)$  in mb/sr.

$E$	$a_0(E)$	$a_1(E)$	$a_2(E)$
237.5	0.4079	0.0524	-0.1803
310.7	8.9528	6.8962	0.7359
332.5	3.5218	-2.7426	-5.5391
367.7	18.60	12.80	-2.6297
427.5	26.80	16.80	-4.8594
461.7	78.20	40.20	-36.40

Table 5: The fitted resonant parameters for the astrophysical  $S$  factor of the  ${}^9\text{Be}(p, \gamma){}^{10}\text{B}$  reaction.

Resonance parameters	Compilation [35]	Zahnow, <i>et. al.</i> [15]	Wulf, <i>et. al.</i> [11]	A.Sattorov, <i>et. al.</i> [7]	Present work
$J^\pi$	$1^-$	$1^-$	$1^-$	$1^-$	$1^-$
$E_1$ [keV]	$287 \pm 5$	$342 \pm 27$	295	296	282
$\Gamma_1$ [keV]	$120 \pm 5$	$297 \pm 27$	145	140	140
$\Gamma^p/\Gamma_1$	0.3		0.3	0.35	0.35
$\Gamma^\gamma$ [eV]	4.8	4.8	1.8	$1.2^a$	1.2
$J^\pi$	$2^{+b}$	$2^+$	$2^+$	$2^+$	$2^+$
$E_2$ [keV]	$892 \pm 2$	$890 \pm 1.8$	890	890	890
$\Gamma_2$ [keV]	$72 \pm 4$	$81.0 \pm 2.7$	79.2	80	83
$\Gamma^p/\Gamma_2$	$\approx 0.65$			0.75	0.75
$\Gamma^\gamma$ [eV]	25.8			$25.8^c$	25.8
$J^\pi$	$0^+$	$0^+$	$0^+$	$0^+$	$0^+$
$E_3$ [keV]	972	972	972	972	957
$\Gamma_3$ [keV]	$2.65 \pm 0.18$				2.7
$\Gamma^p/\Gamma_3$	1.0	1.0	1.0	1.0	1.0
$\Gamma^\gamma$ [eV]	8.5	8.5	8.5	$8.5^c$	6.5
$J^\pi$	$2^-$	$2^-$	$2^-$	$2^-$	$2^-$
$E_4$ [keV]	1161	1265	1215	1196	1196
$\Gamma_4$ [keV]	$210 \pm 60$	$387 \pm 27$	190	290	290
$\Gamma^p/\Gamma_4$ [eV]	$\approx 0.65$		0.72	0.52	0.52
$\Gamma^\gamma$ [eV]	8.5		5.8	$7.9^c$	7.9

<sup>a</sup>This parameter was taken from Ref. [36].

<sup>b</sup>See table 10.16 in Ref. [35] and p.p. 5 and 6 of Ref. [7].

<sup>c</sup>This parameter was taken from Ref. [35].

Table 6: Rates  $N_A \langle \sigma_{ij} v_{ij} \rangle$  of the  ${}^9\text{Be}(p, \gamma){}^{10}\text{B}$  and  ${}^{16}\text{O}(p, \gamma){}^{17}\text{F}$  reactions in the dependence from the temperature  $T_9$  (K) in the unit of  $10^9$ .

$N_A \langle \sigma_{ij} v_{ij} \rangle, \text{cm}^3 \text{mol}^{-1} \text{s}^{-1}$							
$T_9,$	${}^9\text{Be}(p, \gamma){}^{10}\text{B}$			$T_9$	${}^{16}\text{O}(p, \gamma){}^{17}\text{F}$		
K	our work	[21](ratio)	[40](ratio)	K	our work	[21](ratio)	[41](ratio)
1	2	3	4	5	6	7	8
0.010	3.81[-13]	3.87[-13](0.98)	4.29[-13](0.89)	0.010	8.58[-25]	6.73[-25](1.27)	7.20[-25](1.19)
0.011	1.61[-12]	1.64[-12](0.98)	1.81[-12](0.89)	0.011	7.97[-24]	7.10[-24](1.12)	7.58[-24](1.05)
0.012	5.74[-12]	5.90[-12](0.97)	6.47[-12](0.87)	0.012	6.13[-23]	5.71[-23](1.07)	6.08[-23](1.01)
0.013	1.79[-11]	1.85[-11](0.97)	2.02[-11](0.89)	0.013	3.99[-22]	3.68[-22](1.09)	3.91[-22](1.02)
0.014	4.99[-11]	5.18[-11](0.96)	5.64[-11](0.88)	0.014	2.20[-21]	1.97[-21](1.12)	2.09[-21](1.05)
0.015	1.27[-10]	1.32[-10](0.96)	1.43[-10](0.87)	0.015	1.03[-20]	9.06[-21](1.14)	9.60[-21](1.08)
0.016	2.97[-10]	3.10[-10](0.96)	3.35[-10](0.89)	0.016	4.20[-20]	3.65[-20](1.15)	3.87[-20](1.09)
0.018	1.34[-9]	1.41[-9](0.95)	1.51[-9](0.89)	0.018	4.92[-19]	4.30[-19](1.14)	4.54[-19](1.08)
0.020	4.89[-9]	5.17[-9](0.95)	5.50[-9](0.89)	0.020	4.05[-18]	3.59[-18](1.13)	3.77[-18](1.07)
0.025	6.53[-8]	6.99[-8](0.93)	7.32[-8](0.89)	0.025	2.78[-16]	2.50[-16](1.11)	2.62[-16](1.06)
0.030	4.70[-7]	5.08[-7](0.93)	5.24[-7](0.90)	0.030	6.96[-15]	6.32[-15](1.10)	6.59[-15](1.06)
0.040	8.29[-6]	9.11[-6](0.91)	9.15[-6](0.91)	0.040	7.49[-13]	6.89[-13](1.09)	7.16[-13](1.05)
0.050	6.36[-5]	7.05[-5](0.90)	6.94[-5](0.92)	0.050	2.06[-11]	1.91[-11](1.08)	1.98[-11](1.04)
0.060	3.01[-4]	3.34[-4](0.90)	3.24[-4](0.93)	0.060	2.57[-10]	2.39[-10](1.07)	2.48[-10](1.03)
0.070	1.00[-3]	1.15[-3](0.90)	1.11[-3](0.93)	0.070	1.91[-9]	1.79[-9](1.07)	1.86[-9](1.03)
0.080	2.89[-3]	3.18[-3](0.91)	3.05[-3](0.95)	0.080	9.96[-9]	9.37[-9](1.06)	9.71[-9](1.03)
0.090	6.86[-3]	7.50[-3](0.91)	7.16[-3](0.96)	0.090	4.01[-8]	3.78[-8](1.06)	3.92[-8](1.02)
0.10	1.45[-2]	1.57[-2](0.92)	1.50[-2](0.96)	0.10	1.33[-7]	1.26[-7](1.05)	1.30[-7](1.02)
0.11	2.78[-2]	2.99[-2](0.93)	2.85[-2](0.97)	0.11	3.76[-7]	3.57[-7](1.05)	3.70[-7](1.02)
0.12	4.9[-2]	5.31[-2](0.93)	5.06[-2](0.98)	0.12	9.45[-7]	9.01[-7](1.05)	9.31[-7](1.01)

Table 7: Continued Table 4

$N_A \langle \sigma_{ij} v_{ij} \rangle, \text{ cm}^3 \text{ mol}^{-1} \text{ s}^{-1}$							
1	2	3	4	5	6	7	8
0.13	8.35[-2]	8.88[-2](0.94)	8.47[-2](0.99)	0.13	2.15[-6]	2.06[-6](1.05)	2.12[-6](1.01)
0.14	1.34[-1]	1.41[-1](0.95)	1.35[-1](0.99)	0.14	4.51[-6]	4.32[-6](1.05)	4.46[-6](1.01)
0.15	2.05[-1]	2.16[-1](0.95)	2.06[-1](1.00)	0.15	8.83[-6]	8.48[-6](1.04)	8.74[-6](1.01)
0.16	3.05[-1]	3.20[-1](0.95)	3.05[-1](1.00)	0.16	1.63[-5]	1.57[-5](1.04)	1.62[-5](1.01)
0.18	6.16[-1]	6.42[-1](0.96)	6.13[-1](1.01)	0.18	4.81[-5]	4.65[-5](1.03)	4.78[-5](1.01)
0.20	1.13	1.18(0.97)	1.13(1.01)	0.20	1.22[-4]	1.18[-4](1.03)	1.21[-4](1.00)
0.25	3.99	4.08(0.98)	3.93(1.01)	0.25	7.78[-4]	7.57[-4](1.03)	7.77[-4](1.00)
0.30	1.06[1]	1.07[1](0.99)	1.04[1](1.02)	0.30	3.17[-3]	3.09[-3](1.02)	3.17[-3](0.99)
0.35	2.30[1]	2.31[1](0.99)	2.25[1](1.02)	0.35	9.67[-3]	9.44[-3](1.02)	9.67[-3](1.00)
0.40	4.32[1]	4.30[1](1.00)	4.22[1](1.02)	0.40	2.41[-2]	2.36[-2](1.02)	2.43[-2](0.99)
0.45	7.25[1]	7.16[1](1.01)	7.07[1](1.03)	0.45	5.22[-2]	5.09[-2](1.03)	5.25[-2](0.99)
0.50	1.11[2]	1.09[2](1.02)	1.08[2](1.03)	0.50	1.01[-1]	9.84[-2](1.03)	1.01[-1](0.99)
0.60	2.17[2]	2.11[2](1.03)	2.11[2](1.03)	0.60	2.99[-1]	2.90[-1](1.03)	3.01[-1](0.99)
0.70	3.54[2]	3.44[2](1.03)	3.45[2](1.03)	0.70	7.07[-1]	6.83[-1](1.03)	7.12[-1](0.99)
0.80	5.18[2]	5.04[2](1.03)	5.08[2](1.02)	0.80	1.43	1.38(1.04)	1.44(0.99)
0.90	7.11[2]	6.95[2](1.02)	6.98[2](1.02)	0.90	2.59	2.49(1.04)	2.61(0.99)
1.00	9.41[2]	9.20[2](1.02)	9.24[2](1.02)	1.00	4.31	4.13(1.04)	4.34(0.99)
1.25	1.76[3]	1.70[3](1.03)	1.71[3](1.03)	1.25	1.19[1]	1.13[1](1.05)	1.19[1](0.99)
1.50	3.08[3]	2.92[3](1.05)	2.93[3](1.05)	1.50	2.55[1]	2.42[1](1.05)	2.56[1](1.00)
1.75	4.98[3]	4.61[3](1.08)	4.62[3](1.08)	1.75	4.68[1]	4.40[1](1.06)	4.68[1](1.00)
2.00	7.39[3]	6.75[3](1.09)	6.73[3](1.10)	2.00	7.69[1]	7.19[1](1.07)	7.67[1](1.00)
2.50	1.31[4]	1.16[4](1.13)	1.16[3](1.13)	2.50	1.67[2]	1.54[2](1.08)	1.66[2](1.01)
3.00	1.89[4]	1.64[4](1.16)	1.65[4](1.15)	3.00	3.00[2]	2.73[2](1.10)	
3.50	2.42[4]	2.07[4](1.17)	2.09[4](1.16)	3.50	4.77[2]	4.30[2](1.11)	
4.00	2.86[4]	2.46[4](1.16)	2.45[4](1.17)	4.00	6.98[2]	6.24[2](1.12)	
5.00	3.45[4]	2.90[4](1.19)	2.94[4](1.17)	5.00	1.27[3]	1.12[3](1.13)	
6.00	3.76[4]	3.15[4](1.19)	3.18[4](1.18)	6.00	1.99[3]	1.75[3](1.14)	
7.00	3.88[4]	3.29[4](1.18)	3.27[4](1.19)	7.00	2.85[3]	2.49[3](1.15)	
8.00	3.89[4]	3.26[4](1.19)	3.26[4](1.19)	8.00	3.83[3]	3.34[3](1.15)	
9.00	3.84[4]	3.23[4](1.19)	3.20[4](1.20)	9.00	4.90[3]	4.27[3](1.15)	
10.00	3.76[4]	3.24[4](1.16)	3.10[4](1.21)	10.00	6.06[3]	5.27[3](1.15)	